INORGANIC CHEMISTRY
FRONTIERS

REVIEW

View Article Online
View Journal | View Issue

Cite this: *Inorg. Chem. Front.*, 2020, **7**, 2702

Perovskite nanomaterials as optical and electrochemical sensors

Jesna George K,† Vishaka V Halali,† Sanjayan C. G., V. Suvina, M. Sakar and R. Geetha Balakrishna *

The perovskite family is comprised of a great number of members because of the possible flexible substitution of numerous ions in its system. These compounds have a broad range of applications due to their outstanding optoelectronic properties in solar cells, photodetectors, lasers, and light-emitting diodes (LEDs). Perovskite nanocrystals (PNCs) are highly tolerant to defects, unlike metal chalcogenides, and do not require surface passivation to retain high quantum yields. Interestingly, the defect structures and trap states in perovskites are often found only in their conduction and/or valence bands and not in the mid-states of the bandgap. Such characteristics essentially boost their properties and largely favor their sensing applications. Perovskites have thus been attempted by numerous groups to address the serious concern of heavy metal ions, biomolecules, and gas molecule detection with high selectivity and sensitivity limits. In this context, the current review describes recent developments and various strategies used in applying perovskites as probes for sensing various contaminants, drugs, and gases in the environment. The focus is on two main aspects: (i) the exploitation of the high fluorescence of these perovskites for optical sensing and (ii) the utilization of the redox ability of these perovskites for electrochemical sensing. This review also outlines the existing challenges, giving future perspectives for developing perovskite-based sensing probes of high sensitivity and enduring stability for a range of environmental analytes.

Received 10th March 2020,
Accepted 11th May 2020

DOI: 10.1039/d0qi00306a

rsc.li/frontiers-inorganic

1. Introduction

Environmental contamination with heavy metal ions is a severe problem since most of these ions are toxic. Although a few metal ions, namely copper, iron, zinc, and manganese, are nutritionally vital for healthy living, some metal ions such as

Centre for Nano and Material Sciences, Jain University, Jain Global Campus, Bangalore 562112, Karnataka, India. E-mail: br.geetha@jainuniversity.ac.in
†Equal contributors

Jesna George K

Jesna K. G. completed her Master's degree in General Chemistry in the year 2018 and is currently a Junior Research Fellow pursuing her Ph.D. under the guidance of Prof. R Geetha Balakrishna at the Center for Nano and Material Sciences, Jain University, Bangalore, India. She also has experience in synthesizing nanoparticles by green methods, for biological applications. Her other research interests include synthesizing nanomaterials for optoelectronic/sensing technologies and she wishes to develop novel sensors for water contaminants.

Vishaka V Halali

Mrs Vishaka V. Halali obtained her Bachelor's degree from Mount Carmel College, Bangalore University, and her Master's in Chemistry from the Center for Nano and Material Sciences, Jain University, Bangalore. Presently she is working as a Senior Research Fellow and a Ph.D. scholar under the guidance of Prof. R. Geetha Balakrishna at the Center for Nano and Material Sciences, Jain University, Bangalore, India. Her interests are in the design and synthesis of organic probes and inorganic probes for chemical sensing applications.

lead, cadmium, and mercury are hazardous even in trace concentrations. Considering the toxic effects of these metal ions in the environment, there is a continuous demand for the development of highly sensitive sensing strategies for their detection. Numerous analytical approaches, including liquid chromatography, capillary electrophoresis, gas chromatography, spectrophotometry, atomic absorption spectrometry (AAS), inductively coupled plasma atomic emission spectroscopy (ICP-AES), synchronous fluorescence and pH-based flow injection analysis have been established for the determination of such environmental pollutants.[1–5] However, most of these techniques suffer from the drawbacks of low sensitivity, low selectivity, poor stability, being expensive, the use of complicated instruments, requirements for well-experienced professionals, and the pretreatment of the sample, thus making them impossible for real-time and on-site detection. Very few techniques, such as chemosensing, have gained much attention where the determination of analytes can be estimated by the naked eyes.[6] These chemosensors provide easy, safe, effective, on-site, and rapid real-time detection, simply and inexpensively providing both qualitative and quantitative information.[7]

Chemosensors can convert chemical information into a useful signal due to chemical reactions that occur in the analyte, leading to a change in the physical properties of sensor materials. Chemical sensors consist of two major components, namely, a receptor (a molecular recognition system) and a transducer that expresses the connected binding occasions. There are a variety of materials that can be used as chemosensors, namely, polymers, organic molecules and metal oxide nanoparticles, and these are reportedly used for the sensing of different analytes ranging from cations, anions, explosives, biomolecules and gases in diverse fields including biological, medical, defense security and environmental fields.[8–25] To this end, herein, we have highlighted the use of perovskite chemosensors that are highly sensitive to changes in the optical/electrochemical signals that arise from a significant variation in their absorbance, fluorescence or current/voltage.

2. Scope of the review

One can see the reports of various PNCs as sensing probes in the literature.[26–33] In this direction, in 2018, Zhu *et al.* comprehensively reviewed various perovskites for sensing applications, wherein they discussed the perovskite stability under various environmental conditions and demonstrated their use as sensors for diverse analytes like humidity, temperature, gases, explosives, solvents and metal ions.[34] To date, this review paper by Zhu *et al.* is the only comprehensive report on the sensing ability of metal halide perovskites. Since research on perovskites is very rapidly advancing, it is important to study the advances in this field over the last two years. More advances were seen after 2018, especially in the field of metal ion and gas sensing and we intend to provide a brief account of the present status of various perovskite materials used for sensing applications that were reported after the last review in 2018. Fig. 1 provides the number of papers published on sensing metal ions, biomolecules, and gases using PNCs in the last 5 years. As can be seen, only a limited number of research papers have recently been published on sensing biomolecules and gases. Biomolecules cannot be optically sensed by perovskites since their biocompatibility is inherently nil. It has been observed that when a biomolecule is tagged to PNCs, the PNCs lose their structure and fluorescence immediately. However, they show good stability and sensing ability in electrochemical sensing. In this context, this review highlights the biomolecules and gas sensing achieved through an electrochemical method, wherein adsorption and porosity are identified as key influential parameters.

The optical sensing mainly utilizes ABX_3 (X = halide ions)-type perovskites, while electrochemical sensing mainly utilizes ABO_3/ABO_4-type perovskites. Gas sensing involves both ABX_3

Sanjayan C. G.

Mr Sanjayan C. G. obtained his B.Sc. degree from Chettinad Academy of Research and Education and his M.Sc. in Nanoscience and Nanotechnlogy from the University of Madras. Presently, he is working as a Junior Research Fellow at the Center for Nano and Material Sciences, Jain University, and is pursuing his Ph.D. under the guidance of Prof. R Geetha Balakrishna, and Dr Sakar Mohan. His research interests include the synthesis and development of perovskite fluorescent probes for bio sensing.

V. Suvina

Ms Suvina V. is a Senior Research Fellow and a Ph.D. scholar under the guidance of Prof. R Geetha Balakrishna and Dr D. H. Nagaraju at the Center for Nano and Material Sciences. She obtained her Master's degree from Karunya University, Coimbatore. Her area of research mainly focuses on electrochemical sensors. Recently, she was on a student exchange program at National Taipei University of Technology (NTUT), Department of Electro-Optical Engineering, Taiwan. She has published 7 research papers in peer reviewed journals.

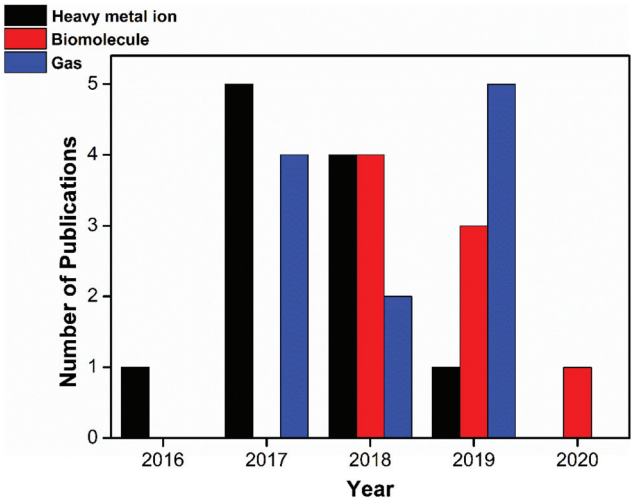

Fig. 1 Statistical data from the literature collected from 2016 to the present on the perovskites being exploited for heavy metal ion sensing, biomolecule sensing, and gas sensing applications.

and ABO_3 type perovskites. Therefore, our review describes the various strategies used in sensing and developments achieved in the last couple of years in this field, with a neat focus on (i) the exploitation of the high fluorescence of these perovskites as optical sensors and (ii) the utilization of the redox capability of these perovskites for electrochemical sensing. Lastly, the current challenges and forthcoming prospectives for sensing probes based on perovskites, in the framework of high sensitivity and enduring stability, are also discussed at length. At this juncture, we believe that this review will provide necessary insights towards achieving high-sensitivity limits and to design stable devices for enhanced sensitivity and sensing over a range of analytes in different environments.

3. Optical sensing

Accordingly, many organic dye-based optical sensors have been established and reported for the sensing of metal ions.[35–40] Organic dyes have limited applications due to their dependency on pH, self-quenching behavior at greater concentrations, impervious Stokes shifts, poor molar absorption coefficients, constricted absorption, and wide emission with indigent separation of absorption and emission bands.[16,41,42]

As an alternative to organic-based dyes, perovskite nanocrystals (PNCs) possess exceptional optical properties that render them as major assets as probes for sensing applications. The basic component of perovskites is the ABX_3 structure and this simple structure consists of corner-sharing BX_6 octahedra, where "A" is a cation or a molecule that is selected to neutralize the total charge, the "B" atom is typically a Pb^{2+} cation and "X" is a halide ion such as Cl^-, Br^- or I^- (Fig. 2).[43] These have been denoted as organic–inorganic hybrid perovskites or all-inorganic perovskites, which is based on whether the "A" site is occupied with an organic molecule or an inorganic cation.[44–47] The family of perovskites comprises a vast number of members because of the flexible substitutions of ions in the ABX_3 structure. These compounds have a broad range of applications including solar cells,[48–50] photodetectors,[51–54] lasers,[55,56] and light-emitting diodes (LEDs)[57–61] due to their excellent optical and electronic properties.[51,62–68]

The remarkably high fluorescence of PNCs confers very high sensitivity when they are used as optical sensors. The ancillary binding of receptor units to the PNC's surface causes

M. Sakar

Dr Sakar Mohan received his Ph.D. from the University of Madras in 2015. Later, he moved to Laval University, Canada for his postdoctoral studies. Currently, he is working as an Assistant Professor at the Centre for Nano and Material Sciences, Jain University, India since 2017. His research interests include photocatalysis, membranes, biodiesel, sensors and biomaterials. To date, his publications include 51 research papers, 5 book chapters and 65 conference papers.

R. Geetha Balakrishna

Prof. Geetha Balakrishna, presently the Director of the "Centre for Nano and Material Sciences", Jain University, is a Professor in Chemistry. Her major areas of research include photochemistry and nanomaterials and she works specifically in the syntheses of numerous nanocomposite materials, membranes and quantum dots, which are active to photons and hence applicable to liquid junction solar cells, sensors, water filtration/purification, disinfection, desalination and metal ion separation. She is a Fulbright fellow and has guided many students in their research projects leading to Doctoral and Post Doctoral degrees. She is a fellow/member of many renowned scientific groups. She has around 108 publications and five patents to her credit and has successfully completed many funded projects of great importance.

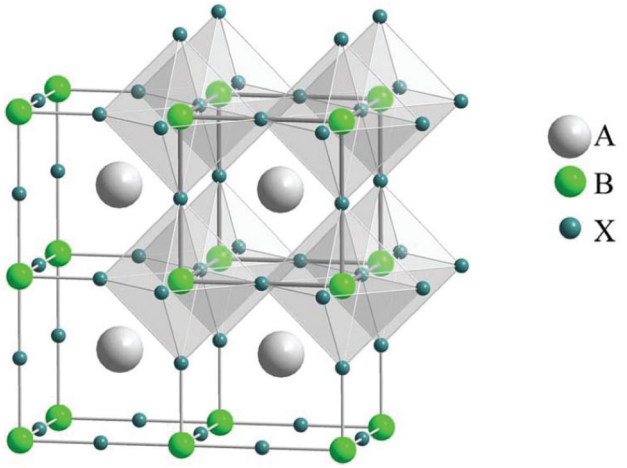

Fig. 2 General crystal structure of the perovskite ABX_3 with evidenced corner-sharing octahedral BX_6 (reprinted with permission from ref. 43. Copyright 2008 APS).

a considerable loss of fluorescence. The generated PNC-ligand conjugate helps in spatial luminescence center separation and the binding sites of the analyte are distinct from the fluorescent probes based on organic dyes. PNCs enjoy the effects of quantum confinement because of their dimensionality and material composition. Marginally different energies arising from the array of nearby transitions will shorten them into a single intense transition. Hence, quantum confinement is responsible for their amazing optoelectronic properties such as long carrier diffusion length, extremely narrow emission bands, and high photoluminescence quantum yields.[16,36–40] With metal ions, the interaction of PNCs gives rise to either the fluorescence quenching or fluorescence enhancement mechanism. In general, the interaction of PNCs with metal ions is a very complicated process and many interaction routes have been reported for the fluorescence quenching mechanism, namely photoinduced electron transfer (PET), non-recombination induced by cation exchange, ligand competition-induced non-radioactive recombination, non-radioactive recombination induced by the electron transfer mechanism, electron transfer *via* binding with surface ligands, inner filter quenching and Förster resonance energy transfer (FRET).[35,69–71]

Optical sensing based on metal chalcogenide (MC) quantum dots has been vastly explored and well established.[72–76] Unlike MC quantum dots, PNCs are highly tolerant of defects and they do not require surface passivation to retain high quantum yields. Interestingly, the defect structures and trap states in PNCs are often found to be located in the conduction and valence bands and not in the mid-states of the bandgap. Compared to metal chalcogenide QDs, all-inorganic perovskite $CsPbBr_3$ QDs can reach quantum yields up to 90% with emission widths as low as 12 nm (ref. 77) and these two are the main boosting parameters for us to utilize their properties for sensing and achieve high detection limits. Also, $CsPbBr_3$ PNCs exhibit absorption that is higher by nearly two orders of magnitude as compared to MCs. The mechanism of optical sensing can be divided into four categories as given below.

3.1 Cation exchange

The cation of the analyte binds to the B site ion on the surface of the sensing perovskite nanocrystal and allows the exchange process, tunes the composition, and repairs the shallow traps on the surface, thereby leading to changes in its optical properties. Passivation of the surface can be understood by adjusting the surface states *via* cation exchange. $CsCuCl_3$ reported by Aamir *et al.* shows excellent optical properties with a bandgap energy of 2.6 eV. These $CsCuCl_3$ perovskites were sensitive to many metal ions, wherein the fluorescence was quenched by Hg^{2+} and Ag^{2+}, but the same was enhanced by Pb^{2+} ions. This implies that $CsCuCl_3$ could be used as a fluorescence "turn-on" chemidosimeter for the selective sensing of Pb^{2+}. By combining the $CsCuCl_3$ and Hg^{2+} ions, they developed a more efficient sensor for Pb^{2+} ion sensing and the possible mechanism for this reaction is shown in Fig. 3(a).[78] A hybrid $CH_3NH_3PbBr_3$ perovskite quantum dot (QD) was used as a fluorescent nanosensor for the rapid visual determination of ultra-trace mercury ions (Hg^{2+}). Noticeably, the PL peak at 520 nm for $CH_3NH_3PbBr_3$ QDs was suppressed by Hg^{2+} and a blue shift in their optical properties was observed with an increase in the amounts of Hg^{2+} and this is attributed to the surface ion-exchange reaction. Good selectivity, sensitivity, and lower LOD (limit of detection) of 0.124 nM (24.87 ppt) in the range of 0 to 100 nM were achieved. Fig. 3(b) shows the PNC structure, wherein the Hg^{2+} ions replace part of the Pb^{2+} ions on the surface of QDs, thereby leading to fluorescence quenching. It was substantiated through XPS analysis that as the concentration of Hg^{2+} increases, the Pb : Br ratio decreases (Hg : Br ratio increases). The interfering metal ions like Cd^{2+}, Pb^{2+}, Na^+, K^+, Zn^{2+}, Ba^{2+}, Mn^{2+}, Cu^{2+}, Mg^{2+}, Ca^{2+}, and Ag^+ did not any show any influence on the fluorescence intensity of perovskite QDs and also a spot plate test was done for the visual detection of Hg^{2+}.[79] One can find only a couple of papers explaining fluorescence sensing based on cation exchange and only one paper quoting anion exchange as a sensing mechanism. The anion exchange mechanism is explained in detail below.

3.2 Anion exchange

One of the most promising features of $CsPbBr_3$ nanocrystals is their broadly tunable emission wavelengths and the entire visible spectrum can be easily accessed by altering the halide composition. Anion exchange reactions are pervasive features of the metal halide perovskite nanochemistry. Park *et al.* established the method for the development of an easy and portable colorimetric sensor based on cellulose by combining it with $CsPbBr_3$ PQDs for ultrafast naked-eye detection of chlorine and iodine ions. $CsPbBr_3$ PQDs-cellulose composites were produced through a sequential hot injection reaction method. These composites show outstanding stability and durability against various environmental surroundings, along with excel-

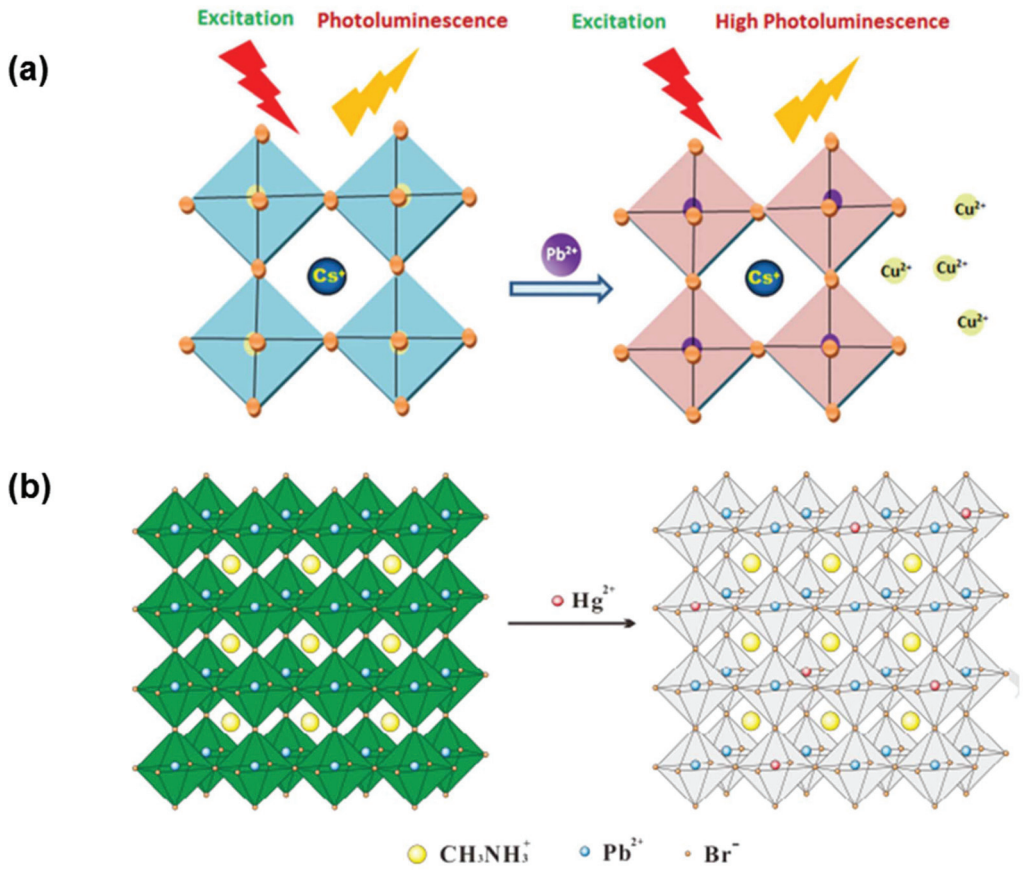

Fig. 3 (a) Possible sensing mechanism of Pb^{2+} by $CsCuCl_3$ (reprinted with permission from ref. 78. Copyright 2016 RSC). (b) Illustration of the cation exchange process on the surface of perovskite quantum dots (reprinted with permission from ref. 79. Copyright 2017 Elsevier).

lent photoluminescence properties. Using the fast anion exchange strategy, iodine and chlorine ions were sensed in real water samples with limits of detection of 2.56 and 4.11 mM, respectively, as shown in Fig. 4.[80]

3.3 Electron transfer

Feasible alignment of the valence band and conduction band energy levels of the donor and acceptor moieties allows electron transfer to occur. Highly photostable fluorescent (XZn) Fe_2O_4 (X = Mg, Mn, or Ni) crystals were ingrained in $BiFeO_3$ nanocomposites for heavy metal ion sensing. These nanocomposites exhibited near-infrared fluorescence responses for XZn or (Fe)–O–O–(Bi) interfaces at 785/832 nm and the (XZn) Fe_2O_4/$BiFeO_3$ lattices showed high/low potentials ranging from 572.15–808.77 meV/206.43–548.1 meV. The obtained data showed that heavy metal ions (Cr^{3+}, Cd^{2+}, Co^{2+}, and Pb^{2+}) hybridized with the paired-spin X–Zn–Fe to decrease the average polarization angles (−29.78 to 44.71°).[81] Because of strong interfacial coupling, the unexpected interfacial electronic transition of Fe_3O_4–$BiFeO_3$ (1.14 eV) created a new electron transfer in the nearby conduction bands or valence bands between Fe_3O_4 and $BiFeO_3$, thus offering a good amount of effective electrons or holes to capture the heavy metal ions on the surface. Also, to enhance the selectivity, interfacial spin-paired orbital alteration by X–Zn co-doping and electron–hole recombination rates was considered. The electron donor state in the Fe_3O_4 spinel is mainly due to superexchange interactions happening between metal ions in the octahedral and tetrahedral lattices. Cation rearrangement takes place *via* the co-doping of X–Zn resulting in the conduction band and valence band being close to the Fermi point. Colloidal $CsPbX_3$ QDs were used as simple promising fast probing material with high sensitivity and selectivity for Cu^{2+} ions in nonpolar solvents like cyclohexane, edible or industrial oils. The detection range was in the order of 2×10^{-9} to 2×10^{-5} M. A small change in PL was explained as a consequence of removing or persuading surface defects in respective metal oleates. However, they used DFT studies to substantiate the observed significant changes in PL during the detection of Cu^{2+}. The observed PL quenching was initiated by the adsorption of Cu^{2+} on the surface of QDs followed by charge transfer. The valence band maximum of perfect $CsPbBr_3$ was donated mainly by Br, whereas the conduction band minimum was contributed dominantly by Pb. Upon the addition of Cu^{2+}, there was the rising of some new states at the valence band maximum edge of $CsPbBr_3$. This feature arose majorly from Cu and somewhat from Br states, allocated to the Br-Cu-OOCH-type formed on the surface of $CsPbBr_3$ QDs. When an exciton is formed, the

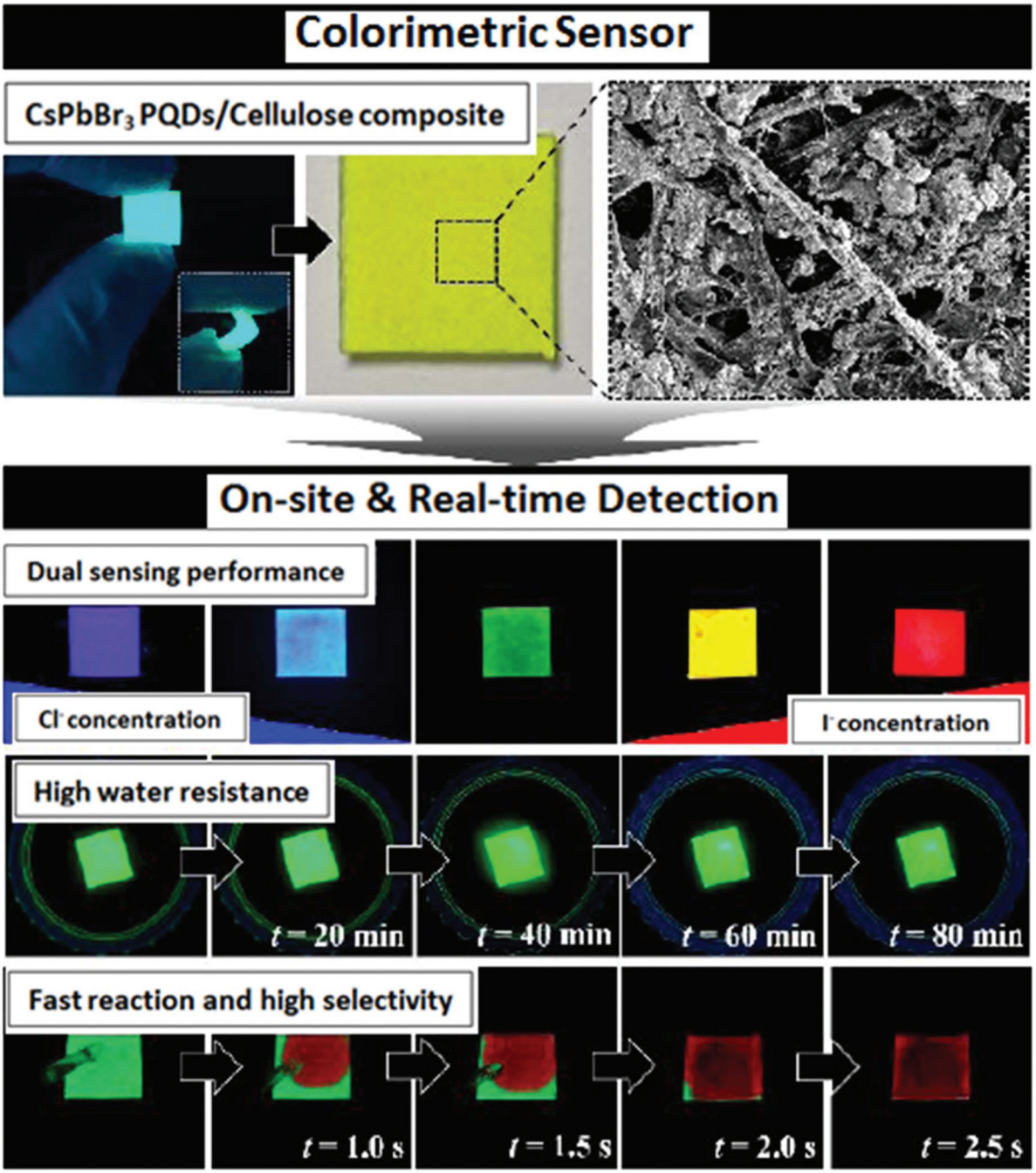

Fig. 4 Schematic representation of iodine-spiked and chlorine-spiked sample determination using $CsPbBr_3$ PQDs-cellulose composites (reprinted with permission from ref. 80. Copyright 2020 ACS).

hole is favored to be taken by these new states as per the principle of minimum energy. This is highly suspected to offer a well-organized nonradiative recombination pathway for the quenching of PL. There is also strong evidence that in addition to the crystal size, structure, and component, the well-defined smooth surface planes of the nanocrystals play a vital role in the sensitive and selective detection of metal ions.[82] $CsPbBr_3$ PQDs were also used by another group as a fluorescent probe for the selective detection of Cu^{2+} in the organic phase (hexane). Quenching of PL intensity on the addition of Cu^{2+} ion was explained on account of electron transfer from the PQDs to Cu^{2+} and the mechanism is supported by the absorption spectrum and PL decay lifetimes. This probe exhibited a detection limit (LOD) of 0.1 nM, a detection range from 0 to 100 nM and high sensitivity of the order 10^7 M^{-1}.[83] Lead-free $Cs_3Bi_2Br_9$: Eu^{3+} perovskite QDs were synthesized *via* an improved ligand-assisted reprecipitation method. The synthesized $Cs_3Bi_2Br_9$: Eu^{3+} perovskite QDs showed emissions,

representing the exciton emission and red emission of Eu^{3+}ions due to efficient electron transfer (ET) from the perovskite QDs to Eu^{3+}. Doping of Eu^{3+} ameliorated the photoluminescence quantum yield (PLQY) from 18% to ~42.4%, in addition to the enhanced water stability of $Cs_3Bi_2Br_9$ perovskite QDs. Eco-friendly and non-toxic $Cs_3Bi_2Br_9$: Eu^{3+} perovskite QDs demonstrated a good linear range from 5 nM to 3 μM with a low detection limit of 10 nM for Cu^{2+} ions in water, and the sensing mechanism is as shown in Fig. 5.[84]

Another typical charge transfer resulting in fluorescence quenching was demonstrated by the Huang and Tan groups. They designed molecularly imprinted polymers (MIPs) through imprinting technology by the sol–gel reaction and used them for the detection of omethoate (OMT) Fig. 6(a) and phoxim Fig. 6(b). The definite interactions between the template and imprinted cavities lead to charge transfer resulting in fluorescence (FL) quenching. MIPs@$CsPbBr_3$ QDs are particularly selective and were found to be a simple fluorescence sensor for the direct detection of organophosphorus (OP) pesticides in real samples such as vegetables and soil.[85,86]

3.4 FRET

Fluorescence Resonance Energy Transfer (FRET) is a non-radiative energy transfer phenomenon. For an effective FRET process, there must be considerable spectral overlap between the emission spectra of the donor and the absorption spectra of the acceptor molecule with the distance between the two spectra being in the range of 10–100 Å. The 2D hybrid perovskite $(NH_3(CH_2)_{10}NH_3)PbBr_4$ was prepared *via* a fast precipitation method and exhibited fluorescence at 552 nm due to aggregation-induced emission (AIE) in a DMSO/H_2O > 4/6 mixed system. The FRET mechanism was demonstrated using rhodamine B (RhB), where RhB acts as a good acceptor as shown in Fig. 7(a). The emission peak of the perovskite $C_{10}PbBrPE$ at 552 nm successfully overlapped with the excitonic peak of RhB with a Förster radius value of 10.37 Å and the donor–acceptor distance was calculated to be 10.21 Å, which was within the range of 10–100 Å. This system was successfully used for the detection of Hg(II) ions in the DMSO/water (1/9) mixed system with a detection limit of 2.36 μM.[87]

In another case, simple perovskite quantum dots (CPBQDs) were used to design a fluorescence resonance energy transfer (FRET)-based detection device. The synthesized CPBQDs improved the FRET detection *via* a nanoscale polymethyl methacrylate (PMMA) fiber membrane ($d \approx 400$ nm) fabricated by the electrospinning method. It was also proposed that it could be used in various fields for detection including biological proteins, metal ions, and pH changes. As a result of the tunable emission spectra of PQDs, there exist many PQDs-fluorescein couples suitable for FRET. This study reveals that electrospinning the polymer fiber membrane with PQDs condensed in it is super sensitive and can act as a multifunctional sensor. The sensing of trypsin was achieved through the cleavage of peptide CF6 (Cys–Pro–Arg–Gly–R6G) and a very low detection limit of 0.1 μg mL^{-1} was obtained. The high-efficiency FRET process between the CPBQD/PMMA FM and cyclam–Cu^{2+} allows a remarkable detection limit for Cu^{2+}, up to 10^{-15} M Fig. 7(b).[88] Table 1 gives the comparison of various perovskite nanocrystals used as optical probes for heavy metal sensing.

3.5 Perovskite sensors in aqueous media

Despite all the struggles and developments made in this area, the instability of perovskites in aqueous media remains a great challenge for their practical applicability as sensors. The perovskite structure collapses due to various environmental factors such as temperature,[27,89] water,[90,91] oxygen,[48,92] *etc*. The tolerance factor has been studied to assess the stability of perovskites. The Goldschmidt tolerance factor (t) is a steadfast empirical key for predicting the stability of the crystal structure. It is determined from the ionic radius of the atoms by using the following expression:

$$t = \frac{r_A + r_X}{\sqrt{2}(r_B + r_X)}$$

where r_A is the radius of the 'A' cation, r_B is the radius of the B cation, and r_X is the radius of the anion. The tolerance value between 0.8–1.0 (Fig. 8) was found to be favorable for the perovskite cubic structure and the non-perovskite structures generally result from a larger (>1) or smaller (<0.8) tolerance factor

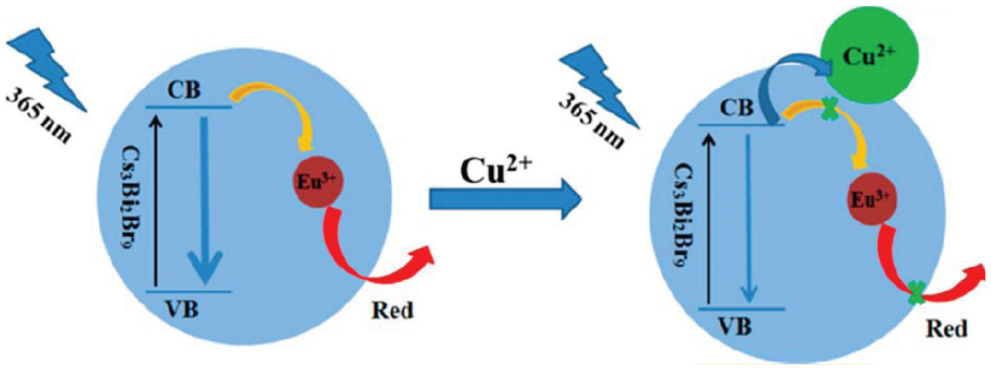

Fig. 5 Schematics of fluorescence quenching due to electron transfer (reprinted with permission from ref. 84. Copyright 2019 ACS).

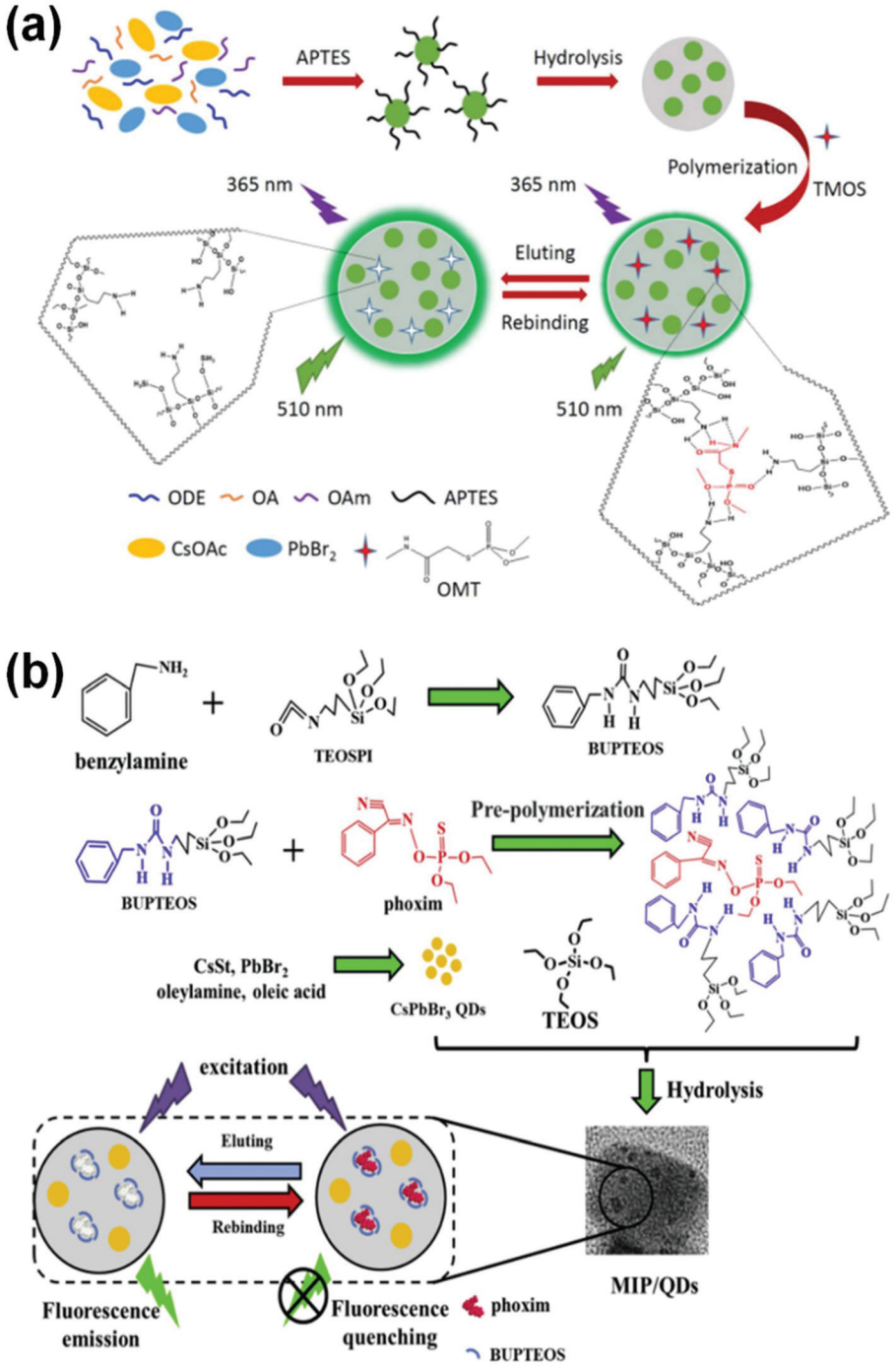

Fig. 6 (a) Graphical representation of a pesticide sensor for the detection of omethoate (OMT) and phoxim (reprinted with permission from ref. 85 copyright 2018 American Chemical Society. (b) Graphical representation of a pesticide sensor for the detection of phoxim (reprinted with permission from ref. 86. Copyright 2019 Elsevier).

value.[93–95] Over the past few years, various methods have been established to improve the stability of perovskites by coating the perovskite surface with hydrophobic materials like acid–base additives,[96,97] alkyl phosphonic acid ω-ammonium chlorides,[98] metal–organic frameworks (MOFs),[99,100] polymers like poly(ethylene glycol) (PEG),[101] poly(vinylpyrrolidone),[102,103] stearic acid,[104] capping them with organic ligands such as PCBEG and PEG-[60]fullerenes.[105,106] These modifications not only help in improving the stability of the perovskite but also support in passivating their trap sites and defect sites,[28,107–117] and this supports better sensitivity when used as sensing probes.

The synthesis of stable 2D PEA_2PbI_4 (where PEA is phenethylammonium) PNCs by the antisolvent precipitation

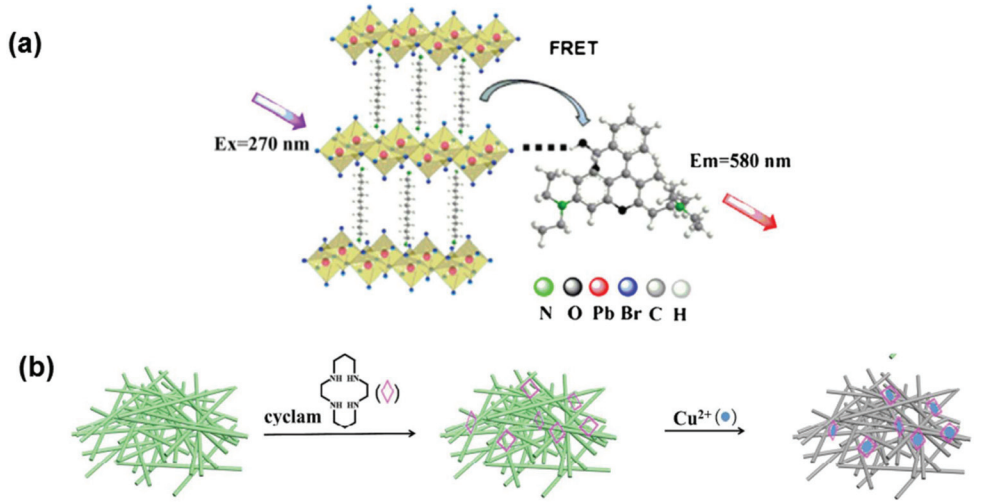

Fig. 7 (a) A possible sensing mechanism for FRET between C_{10}PbBrPE and RhB (reprinted with permission from ref. 87 copyright 2017 Springer). (b) schematic illustration of the sensing of Cu^{2+} using CPBQDs/PMMA FM and cyclam by the FRET mechanism (reprinted with permission from ref. 88 copyright 2013 RSC).

Table 1 Comparison of the LODs of various perovskite nanocrystals used as optical probes for heavy metal and anion sensing

S. no.	Perovskite material	LOD	Analyte	Ref.
1	$CsCuCl_3$	1×10^{-7} M–1.5×10^{-6} M	Pb^{2+}	78
2	$CH_3NH_3PbBr_3$ QDs	0.124×10^{-9} M	Hg^{2+}	79
3	$(XZn)Fe_2O_4$-$BiFeO_3$	—	Co^{2+}, Cr^{3+} & Cd^{2+}	81
4	$CsPbBr_3$	2×10^{-9} M–2×10^{-5} M	Cu^{2+}, Yb^{2+}	82
5	$Cs_3Bi_2Br_9$: Eu^{3+}	5×10^{-9} M–3×10^{-6} M	Cu^{2+}	84
6	$CsPbBr_3$	0.1×10^{-9} M	Cu^{2+}	83
7	$(NH_3(CH_2)10NH_3)PbBr_4(C_{10}PbBrPE)$	2.4×10^{-6} M	Hg^{2+}	87
8	CPBQDs/PMMA FM	0.1×10^{-6} M	Cu^{2+}	88
9	2D PEA_2PbI_4	5×10^{-10} M–5×10^{-2} M	Cu^{2+}	118
10	$CH_3NH_3PbBr_3$	20×10^{-5}–200×10^{-5} M & 2×10^{-3}–100×10^{-3} M	Cu^{2+}&Cd^{2+}	119
11	$CH_3NH_3PbBr_3$	3.2×10^{-6} M	F^-	120
12	$CsPbBr_3$/Cellulose Composite	4.11×10^{-3} & 2.56×10^{-3}	Cl^- & I^-	80

method has been reported by Ma *et al.* It was witnessed that the degradation of PEA_2PbI_4 PNCs in water was due to the process of desorption, where the PEA^+ species desorbed from PbI_2. PNCs could be stabilized in high PEA^+ concentration (>0.15 M) aqueous solutions because of an adsorption process. These two procedures were modest and could attain balance in 0.15, 0.25, and 0.5 M PEA^+ aqueous solution. More significantly, the recyclability of the desorption and adsorption processes was confirmed and it was stable for 2 months. Based on this, the inherently unstable PNCs were stabilized and were utilized practically as a probe for sensing Cu^{2+} in an aqueous environment.[118] Zhang *et al.* attempted a two-step method to encapsulate perovskite $CH_3NH_3PbBr_3$ QDs into a MOF-5 matrix to improve the stability of luminescent perovskite QDs as shown in Fig. 9(a). Outstanding water resistance, thermal stability, and stable photoluminescence were achieved over a wide range of pH and applied to Cu^{2+} and Cd^{2+}. The detection of Cu^{2+} concentration in the range from 20×10^{-5} to 200×10^{-5} M was demonstrated. The luminescence intensity was significantly quenched by the addition of Cu^{2+} ions. For Cd^{2+} ions, the PL intensity was progressively enhanced with increasing concentration of Cd^{2+} ions from 2×10^{-3} to 100×10^{-3} M.[119] Various ligands and their combinations were tried by different researchers to enhance stability. Dual ligands AH (6-amino-1-hexanol) and OA (*n*-octylamine) were used for the synthesis of the $CH_3NH_3PbBr_3$ PQDs probe. Quenching of fluorescence was observed in the presence of F^- ions, due to hydrogen bonding between the hydroxyl groups of AH and F^- ions, and that reduced the growth of the dual ligand-capped perovskite quantum dots (DL-PQDs). This probe showed promising sensitivity and selectivity for the detection of F^- with a limit of detection of 3.2 μM (0.061 mg L^{-1}). A spot plate test was also done for the visual detection of fluoride ions as shown in Fig. 9(b).[120]

4. Electrochemical sensing

Electrochemical sensors are considered to be rapid, low-cost, portable, and user-friendly devices for monitoring environ-

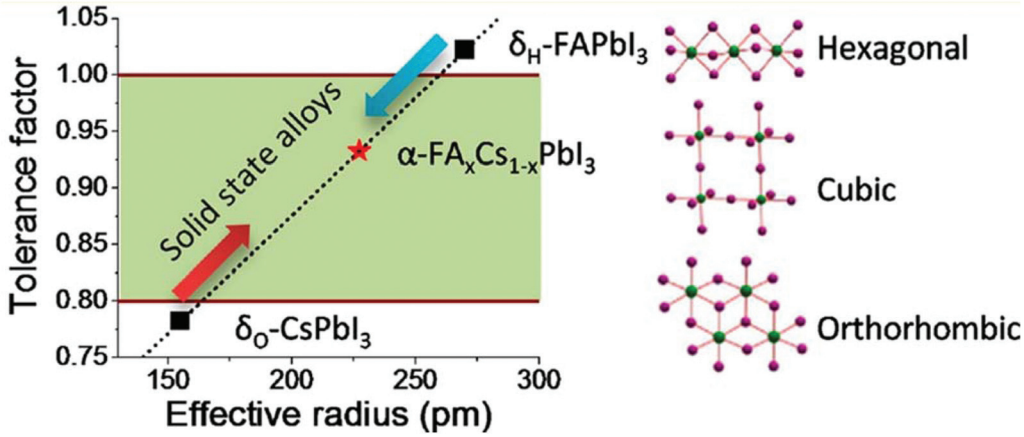

Fig. 8 Correlations between the tolerance factor and the crystal structure of perovskite materials (reprinted with permission from ref. 95. Copyright 2015 ACS).

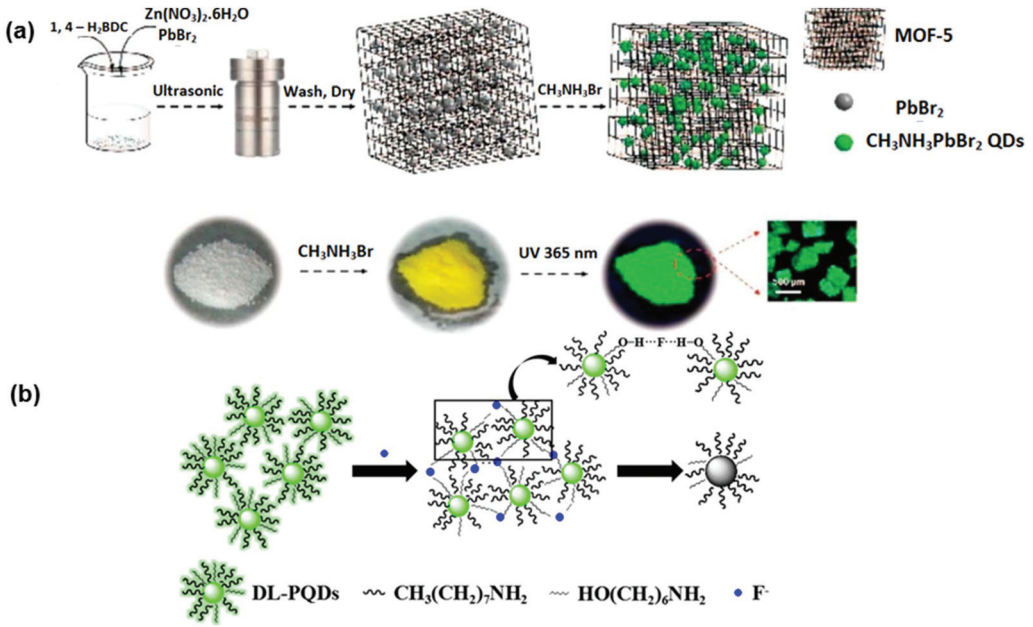

Fig. 9 (a) Schematic representation of the two-step approach to stabilizing PQDs before sensing Cu^{2+} in aqueous media (reprinted with permission from ref. 119. Copyright 2018 ACS). (b) Schematic illustration of the sensing mechanism of F^- by DL-PQDs (reprinted with permission from ref. 120. Copyright 2018 Elsevier).

mental pollution.[121,122] Electrochemical methods are applicable for the detection of environmentally emerging contaminants at ultra-low concentrations with high sensitivity and low detection limits.[123] The method also offers enormous advantages such as high sensitivity, on-site determination, and good selectivity as compared to other methods.[122,124] To detect environmentally toxic metal ions, an electrochemical technique called anodic stripping voltammetry (ASV) is commonly used, wherein high sensitivity, a very low detection limit, and simultaneous detections are achieved.[125]

During the accumulation process, the analyte in the supporting electrolyte solution will be deposited on the surface of the working electrode in the form of film at negative potentials where the oxidation takes place $M_{(s)} \leftrightarrow M^{n+}{}_{(aq)} + ne^-$.[125] The analyte reoxidizes and strips back into the supporting electrolyte solution[125,126] during the stripping process. Similarly, the inorganic perovskite nanocrystals, possessing electrically energetic structures and suitable magnetic and dielectric characteristics, have been broadly used in the development of electrochemical sensors, solid fuel cells, and many of electrochemical catalytic processes.[127] Perovskite materials possessing the ABO_3 and A_2BO_4 structures have been considered for such catalytic and electrocatalytic properties, where the A-site cation is generally occupied by alkaline-earth or rare-earth metal

cation(s), while the B-site cation is normally occupied by transition metal cation(s).[128,129] Both ABO_3 and A_2BO_4 nano-perovskites have been widely used in different applications due to their fascinating properties.

Perovskites of ABO_3-type binary metal oxides are reported to offer high ionic and electronic conductivity, enhanced catalytic activity, thermal and chemical stability, variations in oxygen content, mobility of oxide ions within the crystal, and electrically active structure.[127,130] The probability of substituting the original A-site and B-site cations of perovskite oxides with other metal cations to produce an altered perovskite oxide composition with the formula of $A_{1-x}A'_xB_{1-y}B'_yO_3$ has unlocked the chance to project new functional perovskite oxide compositions.[129] Among them, the alkaline-earth metals (*i.e.*, Ca, Mg, Ba, Sr)-based perovskite materials can be easily formed; they willingly react and are low-cost materials. Therefore, they can conceivably act as electrode materials in electrochemical sensing procedures to sense chemicals and biomolecules in both liquid and gaseous phases.[131] Also, the metal titanates have attracted substantial consideration for their exceptional properties like nontoxicity, chemical stability, low cost, and thermal stability. Their nanocomposites are reported to be excellent electrode materials, even though they suffer from aggregation tendencies. In this respect, assimilating metal titanates into a highly conductive matrix has been demonstrated as a valued approach to improve conductivity and electrocatalytic activity.[132]

4.1 Lanthanide-based perovskite oxide sensors

The $NdFeO_3$ perovskite screen-printed carbon electrode was developed for the electrochemical sensing of dopamine (DA) and uric acid. The $NdFeO_3$, which was modified on a screen-printed carbon electrode, showed better performance as compared to the bare electrode and other perovskite-based sensors, namely $SrPdO_3$,[133] $LaCoO_3$,[134] $LaFeO_3$.[135] They demonstrated that the proposed $NdFeO_3$ perovskite material acts as a modifier for fabricating enzyme-free electrochemical sensors and monitors the biochemical substances.[128] The same perovskite was also tested for AML (amlodipine) sensing by Nada *et al.* by the modification of carbon paste (CP) with $NdFeO_3$, CNTs, and glycine in the presence of SDS. The probe was used for the instantaneous sensing of antihypertensive and antioxidant drugs, AML and AA (ascorbic acid), respectively. The systematic performance of the suggested surface towards AML was examined in terms of linear dynamic range, detection limit and sensitivity. The utilization of the proposed method for AML determination in marketable tablets and human urine has been demonstrated.[127] The proposed nanosensing electrode with combined fascinating characteristics of $NdFeO_3$ nano-perovskites is shown as a reliable alternative to other chromatography and spectroscopy techniques. This study also indicated the potential applicability of this perovskite sensor to other drugs. Akbari *et al.* described the preparation of a new graphene oxide-$LaMnO_3$-modified GCE for the electroanalysis and determination of hydroquinone (HQ) and catechol (CT) and they also showed the excellent performance of this sensor towards the simultaneous determination of HQ and CT by the voltammetry technique.[136] A nanocomposite of lanthanum cobalt nitrate and hydrotalcite nanotubes (LCO/HNT) was designed previously by our group for the detection of flutamide.[124] The developed electrode showed a better electrocatalytic effect on flutamide due to its significant properties such as short electron transfer pathway, large surface area, and superior electron conductivity with the benefits of low cost, rapid detection, trace-level LOD, high detection sensitivity, good reproducibility, excellent stability, and accuracy. The developed electrode achieved a detection limit of 0.002 μM and sensitivity around 0.7571 μA μM^{-1} cm^{-2}.

4.2 Strontium-based perovskite oxide sensors

A fiber-based electrochemical sensor towards Acetominophen (AP) sensing was fabricated using a CeBiO*x* nanofibers-altered screen-printed electrode (SPE). The CeBiO*x* nanofibers were synthesized by electrospinning a precursor solution of polymer using cerium nitrate and bismuth nitrate followed by calcination to decompose the polymer and transform the precursor nanofibers into CeBiO*x* NFs. The obtained results revealed that the Ce : Bi molar ratios in the originators had a noteworthy effect on the electrocatalytic activity of CeBiO*x* towards AP detection. The CeBiO*x*NFs with the optimum Ce : Bi molar ratio showed ultrasensitivity of 360 μA mM^{-1} cm^{-2} and 350 μA mM^{-1} cm^{-2}, with a good detection limit of 0.2 μM and 1 μM (S/N = 3) and a wide linear range up to 130 μM and 500 μM for DPV and CV-based AP detection, respectively, as shown in Fig. 10.[121] Cao *et al.* also detected AP in commercial tablets and spiked human serum samples using these electrodes but with much better accuracy and good recovery.[137]

Systematic characterization of the perovskite oxide family with various compositions of $Pr_{1-x}Sr_xCoO_{3-\delta}$ (x = 0, 0.2, 0.4, 0.6, 0.8, and 1) has been reported and applied for the detection of PPD (P-Phenylenediamine). A correlation was found between the yields of the hydrogen peroxide intermediate (HO_2^-) and the B–O (B-site metal cation to oxygen anion) bond strengths of these perovskite oxides. $Pr_{0.8}Sr_{0.2}CoO_{3-\delta}$ (PSC82) displayed the highest sensitivity to PPD as it produced the highest current due to the HO_2^- yield of 86% that was generated as a result of the chemical oxidation of PPD to *p*-quinone diamine as shown in Fig. 11. Relative to the conventional ultraviolet-visible spectrophotometry (UV-vis) detection method, the amperometric detection of PPD in hair dye using this perovskite sensor provides greater accuracy, higher selectivity toward PPD, and stability, which warrant its potential application to real hair dyes.[129] Table 2 gives a list of different perovskite materials used for sensing various environmental pollutants.

Sundaresan *et al.* synthesized strontium cerate nanoparticles (SC NPs) through a simple sonochemical method called ultrasound-assisted (UA) and stirring-assisted (SA) synthesis (UASC NPs) and applied them as an improved electrode material for the determination of nifedipine (NDF). Interestingly, the UASC NPs-modified screen-printed carbon electrode (UASC NPs/SPCE) showed brilliant electrocatalytic

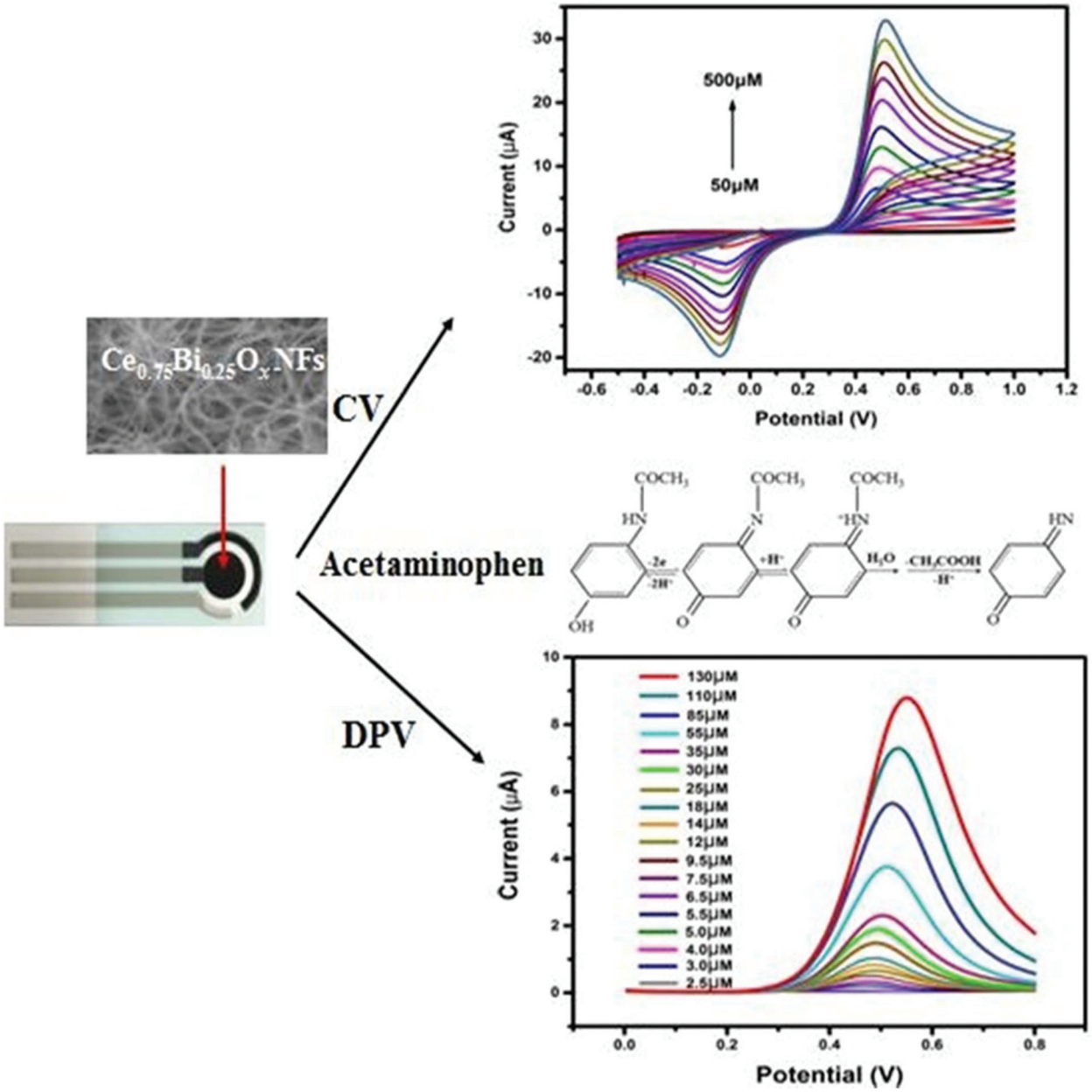

Fig. 10 Representation of an electrochemical sensor for detecting the pain reliever/fever reducer drug Acetaminophen based on an electrospun CeBiO*x* nanofibers-modified screen-printed electrode (reprinted with permission from ref. 121. Copyright 2017 Elsevier).

activity and substantial electroanalytical performance in NDF sensing when compared to SASC NPs/SPCE and unmodified SPCE as shown in Fig. 12.[130]

The synthesized UASC NPs displayed excellent selectivity even in the presence of nitro groups comprising drugs, pollutants, biological compounds, and common inorganic species. They have been effectively used in the sensing of NDF (Nifedipine) in real urine, water, and NDF tablets. The easily accessible and environmentally friendly sonochemical technique offers a facile and operational method for scale control in industry. Strontium-based perovskite $SrZrO_3$ cubes entrenched on nitrogen-doped reduced graphene oxide (N-rGO/$SrZrO_3$) was prepared for the electrochemical sensing of hydroquinone (HQ). The sensor had a good detection limit (0.61 μM), repeatability, reproducibility, and high selectivity towards the sensing of HQ. Therefore, inorganic perovskite oxide-based nanocomposites are realized to be promising for achieving enhanced electrochemical sensitivities.

5. Gas sensing and device fabrication

We would like to highlight that to the best of our knowledge, this review is the first of its kind to summarize and analyze the

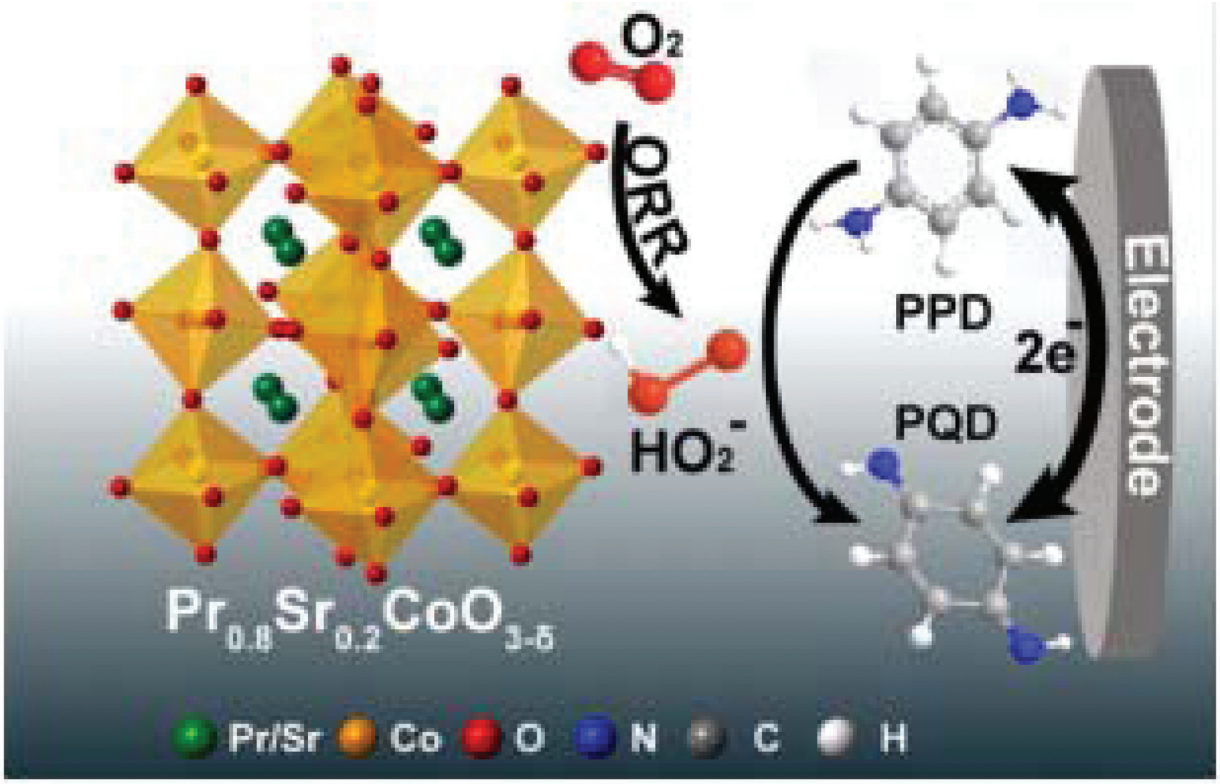

Fig. 11 Schematic representation of the oxygen reduction reaction and the related redox reaction converting PPD into perovskite quantum dots and *vice versa* on the surface of the PSC82/GE electrode (reprinted with permission from ref. 129. Copyright 2019 Elsevier).

Table 2 Comparison of different perovskite electrode materials used for sensing environmental pollutants and drugs with their obtained LODs

S. no.	Electrode material	Technique	Sensitivity	LOD	Linear ranges (μM)	Analyte	Ref.
1.	$NdFeO_3$	SWV	—	0.27 μM	0.5–100 & 150–400	Dopamine	128
2	PSC82	CA	655 μA μM^{-1}	0.17 μM	0.5–100 μM	P-Phenyl diamine	129
3	GLNFCNTCP	DPV	113.2 μA μM^{-1}	0.704 nM	0.003–0.2	AML	127
4	$SrCeO_3$	DPV	1.31 μA μM^{-1}	6.4 nM	0.02–174	NDF	130
5	$LaMnO_3$	DPV	0.0719 μA μM^{-1} and 0.0712 μA μM^{-1}	0.06 μM and γ0.05 μM	0.5–433.3 & 0.5–460.0	HQ & CT	136
6	CeBiO*x*	DPV	360 μAm M cm^{-2}	0.2 μM	0–130	AMP	137
7	$HNT/LaCoO_3$	DPV	0.7571 μA μM^{-1} cm^{-1}	0.002 μM	0.009–145	Flutamide	124
8	$N\text{-}rGO/SrZrO_3$	SWV	—	0.61 μM	25–2500	Hydroquinone	138

use of perovskites for gas sensing, reporting the works published after 2017. It is largely reported that the working of these gas-sensing perovskite devices is based on two concepts: (i) the electron transfer mechanism and (ii) the adsorption mechanism. When the analyte gases like NO_2, CO, O, O_3, H_2S and H_2 are exposed to the applied current/voltage, an interaction between the gas and the electrons results in the formation of reactive oxygen/intermediate species (ROS), which undergo reduction to molecular oxygen $O^{2-} \rightarrow \frac{1}{2}\,2O_2 + 2e^-$. The physicochemical adsorption of this molecular oxygen on the perovskite layer allows changes in electrochemical signals and facilitates sensing.

5.1 O_2 sensing

The sole sensing of oxygen molecules is relatively easy and many groups have attempted it, even much earlier than 2017. The sensing of oxygen gas has reached very high sensitivity levels with perovskite sensing electrodes. In 2017, the nanostructured organometal halides-based perovskite films were fabricated by the spin coating method through a solvent annealing process at 100 °C to detect O_2. In this study, O_2 sensing was carried out using a gold integrated reference electrode based on the resistive response of the device to the exposed O_2 gas. The very sensitive response of the device was

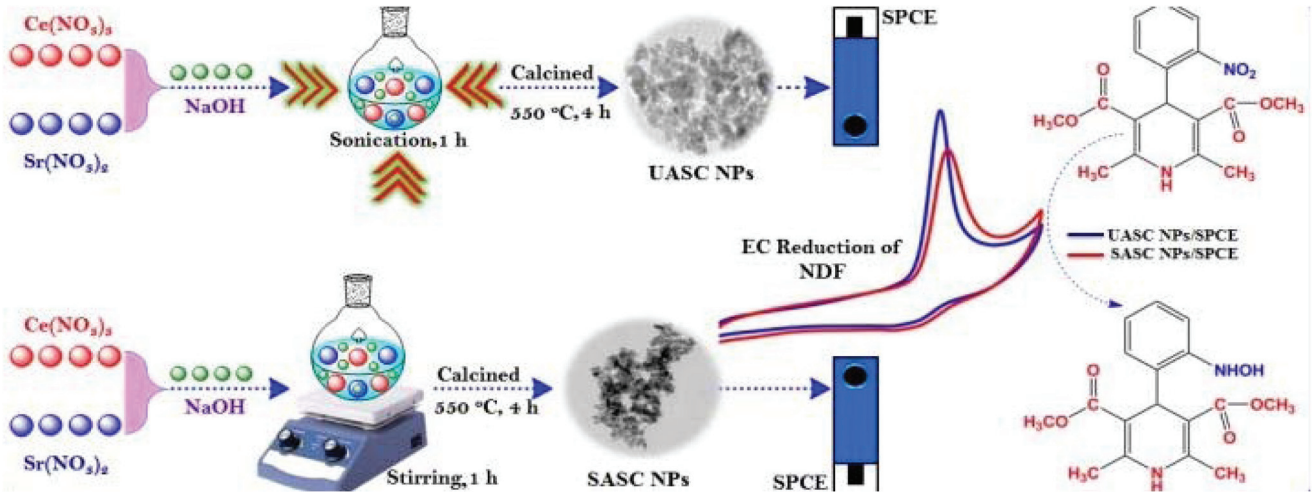

Fig. 12 Synthesis procedures and their electrochemical applications of UASC NPs and SASC NPs towards the sensing of NDF (reprinted with permission from ref. 130. Copyright 2019 Elsevier).

observed at a concentration of 28 ppm in ambient conditions.[139] Another group in 2017 developed a $CH_3NH_3PbI_{3-x}Cl_x$ perovskite coated on a pre-patterned Pt electrode by the spin coating method for self-powered ozone sensors. This sensor could be operated at room temperature and could detect very low concentrations of ozone gas by an electrochemical mechanism. The device achieved remarkable sensitivity at 2500 ppb level of ozone when exposed for 60 min. The developed device exhibited long-term stability and compatibility and could be further used for other analytes.[140]

5.2 H_2, H_2S, and CO sensing

Following O_2, the sensing of H_2S, H_2, and CO gas was largely attempted. In this direction, Ag-doped $CaCu_3Ti_4O_{12}$ (CCTO) films were fabricated as sensor probes to detect H_2S gas. Firstly, the perovskite was synthesized *via* the sol–gel method and the Ag-doped CCTO films were fabricated by a spin coating method. A photolithographic process was applied to deposit positive photoresist on CCTO film by sputtering chromium and gold layers on the substrate and further baking at 400 °C to remove the leftovers from the surface. The obtained results showed that the Ag-doped CCTO responded successfully to the H_2S concentration range between 0.2 and 10 ppm, which was higher than undoped CCTO films. These results proved that Ag acts as a catalyst to improve the sensitivity response of the H_2S sensor. This study also revealed that the exposure of H_2S to the CCTO film allowed its reaction with a reactive oxide layer and resulted in a decrease in the resistivity of the device. The overall mechanism was explained as follows:[141]

$$2H_2S_{ads} + 3O_2{}^-{}_{ads} \rightarrow 2SO_2 + H_2O + 3e^-$$

The Zhang group in 2017 developed the LSCF/YSZ/Pt sensor to detect H_2 gas by an electrochemical method. LSCF (La, Sr)(Cr, Fe) $O_{3-\delta}$ perovskite was synthesized by the sol–gel method and used for sensing H_2. A Pt electrode was used as a reference electrode with YSZ as a solid electrolyte. The interface reaction between H_2 gas and the LSCF/YSZ/Pt sensor resulted in a fast electrochemical response, of −55.4 mV at a low concentration of H_2 gas (100 ppm) and −143.6 mV at 1000 ppm of H_2 gas. It was reported that the oxidation based on the electron donation followed by adsorption facilitated the sensing process in the device. Response time was as low as 4 s and a recovery time of 24 s was obtained for 500 ppm. The probe showed excellent selectivity to hydrogen against the interference of CH_4, C_3H_8, CO, NO_2, and NH_3. The H_2 determination performance for concentrations above 100 ppm is attributed to the high electrocatalytic activity of the perovskite electrode to H_2 oxidation.[142]

La_2CuO_4 doped with strontium, cerium, and zirconium to form $La_{1.9}Sr_{0.2}Ce_{0.1}Cu_{0.8}Zr_{0.2}O_4$ perovskite structure *via* a polymer precursor method was tried for the detection of carbon monoxide (CO). The response of a thick-film device prepared by a screen printing technique was investigated by an AC impedance method using an LCR meter at 300–600 °C. They found that the $La_{1.9}Ce_{0.1}CuO_4$ thick-film device responded well to CO between 50 and 600 ppm at 400 °C, and 50 Hz. The donation of electrons caused oxidation of CO as described in the following equations:

$$O_2 + 2e^- \leftrightarrow 2O^-{}_{ads}$$

$$O_2 + e^- \leftrightarrow O^{2-}$$

$$CO + O^- \rightarrow CO_2 + e^-$$

$$CO + O^{2-} \rightarrow CO_2 + 2e^-$$

Under atmospheric pressure and at high temperatures such as 400–500 °C, the oxygen molecules react or become adsorbed on the oxide surface as O^- or O^{2-}. As a result, the electrons arrested by the adsorbed oxygen were free and contributed to the p-type cuprates, which in turn increased the sensor resistance, thereby decreasing the electric charge to decrease the sensor capacitance.[143]

A novel CO sensing device using bismuth ferrite as a sensing electrode and Au as a reference electrode for environmental monitoring was developed by Chakraborty and group. The obtained detection results confirmed the response of the CO gas to the applied current voltage. The device achieved the lowest detection limit of 30 ppm for CO gas at 350 °C, and the device was stable up to 150 days. The adsorption of O_2 on the sensing surface allowed the ionization of oxygen into O^-, O^{2-} and O^{2-} forms. When CO molecules interacted with this sensing platform, it resulted in the formation of CO_2 and the generated electrons recombined with holes, which in turn increased the resistance.[139]

The effect of the TiO_2/LSCNO (La, Sr, Co, Ni, O) PN heterojunction was investigated for the better sensing capacity of CO gas. The sensitive response of the device was observed at 200 °C for a concentration of 400 ppm. The oxygen vacancies resulted in the enhanced adsorption of CO, which then formed CO_3 and decreased the resistance of the device.[144]

5.3 NO sensing

Among the different target gas monitoring, the determination of nitric oxide (NO) has gained substantial interest. NO is an exceedingly toxic oxidizing gas with a pungent odor. It is continuously released as automotive exhaust and also when there is an influence of nitric acid on metals, such as in metal etching and pickling. It plays an important role in human biological processes like the cardiovascular[145] and immune systems.[146] NO also disturbs the neuron operation, which leads to neurodegenerative diseases.[147] Thus, it is very important to develop NO gas sensors. Many research groups have used perovskites to sense NO_2 gas. For the first time, the Zhuang group in 2017 reported the synthesis of perovskite films *via* the solution processing approach for sensing gases. The $CH_3NH_3PbI_{3-x}$ (SCN)x-based chemiresistor-type sensor was fabricated by spin coating of the perovskite on the Pb $(SCN)_2$, Si/SiO_2 substrate, which can sensitively and selectively detect acetone and nitrogen dioxide (NO_2) at room tempera-

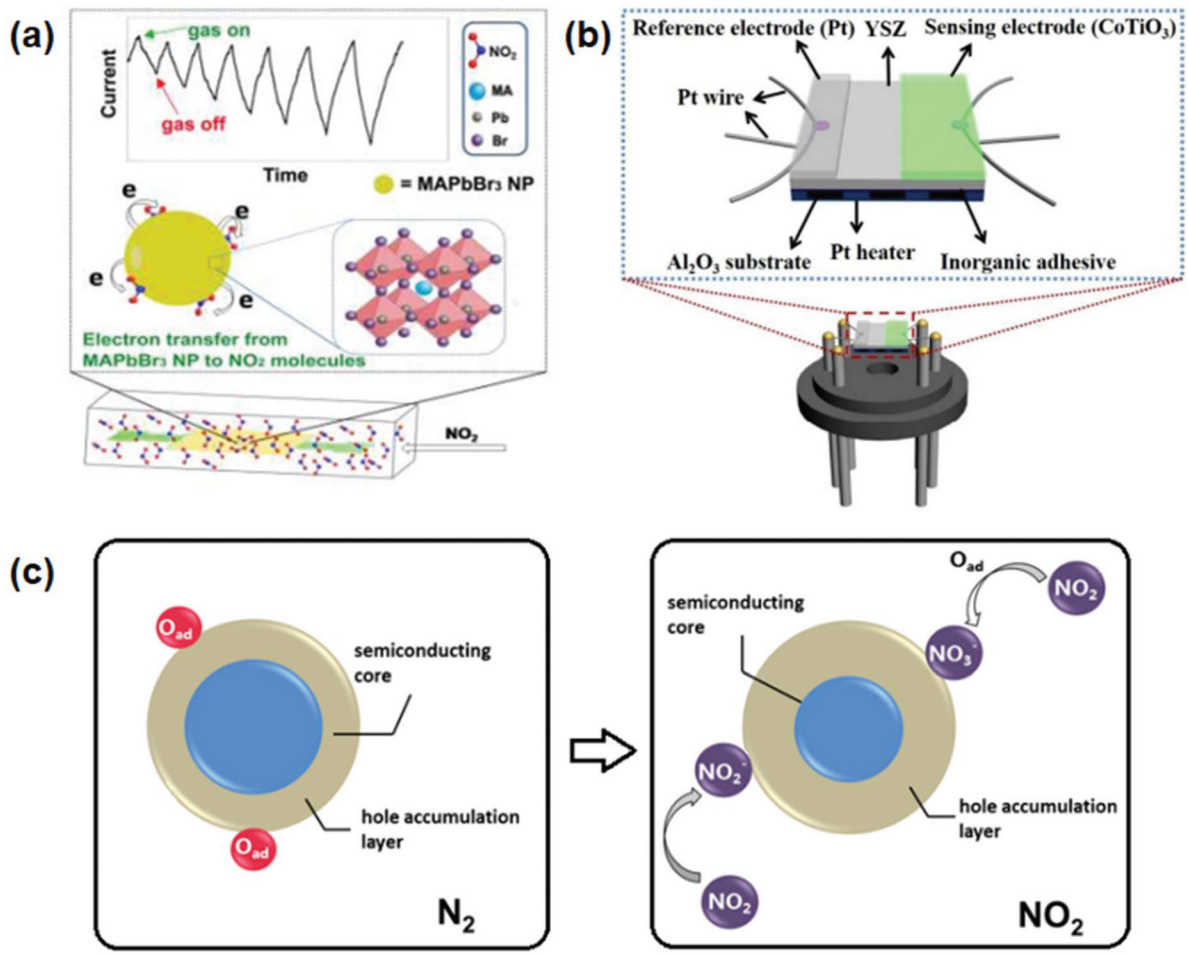

Fig. 13 (a) High-performance room-temperature NO_2 sensors based on $CH_3NH_3PbBr_3$ semiconducting films: the effect of surface capping by alkyl chains on sensor performance (reprinted with permission from ref. 148. Copyright 2019 Elsevier). (b) Schematic view of the planar type YSZ-based NO_2 sensor (reprinted with permission from ref. 149. Copyright 2019 Elsevier). (c) Schematics showing the NO_2 sensing mechanism (reprinted with permission from ref. 150. Copyright 2019 Elsevier).

Table 3 Comparison of detection limits of various perovskite materials used for gas sensing

S. no.	Perovskite	Electrode	LOD (ppm)	Analyte	Ref.
1	$CH_3NH_3PbI_3$	Gold interdigitated electrodes	20	NO_2	153
	$CH_3NH_3PbBr_3$	Gold interdigitated electrodes	0.1		148
	$CoTiO_3$	Pt	50 and 100		154
	$LaFeO_3$	Ag	1		155
	$LaFePd0.05O_{3+}$	Pt	10		151
	$NaBiTiO_3$	CuO	50		152
2	$MAPbI_3$	Gold interdigitated electrodes	28	O_2	139
3	La_2CuBO_4	Gold interdigitated electrodes	50	CO	143
	$BiFeO_3$	Au	30		156
	$LaSrCoNiO_3$	Ag	400		157
4	$CaCu_3Ti_4O_{12}$	Interdigitated gold electrodes	0.2 to 10	H_2S	141
5	(La, Sr)(Cr, Fe)$O_{3-\delta}$	Pt	100	H_2	158

ture. The reference electrodes (Au) were fabricated by photolithography techniques with controlled width and gaps between the adjacent fingers. Sensing occurs based on the increase in the capacitance of the sensing layer to the applied NO_2 gas. The fabricated device sensitively detects NO_2 gas and acetone with the limit of detection of 20 ppm and 200 ppb, respectively, and they confirmed that the sensitivity and stability of the perovskite were increased by thiocyanate and could be widely used for various other gas sensing applications.[136] The same hybrid perovskite ($CH_3NH_3PbBr_3$) but with a different halide were fabricated as semiconducting films under room conditions by a very simple coating technique to detect NO_2 gas up to a limit of 0.1 ppm. The interaction of perovskite film with NO_2 resulted in electron transfer from one to the other, decreasing the conductivity of the perovskite layer. A schematic representation of the device is represented in Fig. 13(a).[148]

A YSZ coupled $CoTiO_3$ electrode was used for sensing NO_2 at the operating temperature of 650 °C. The NO_2 sensor provided a low detection limit of 500 ppb, and the response values were 118 mV and 130 mV towards 50 ppm and 100 ppm NO_2 at 650 °C, respectively; the device was reported to be stable for 20 days. Both the cathodic and anodic reactions were carried out simultaneously when the sensor was exposed to NO_2 gas (cathodic reaction: $NO_2 + 2e^- \rightarrow NO + O^{2-}$ and anodic reaction: $O^{2-} \rightarrow \frac{1}{2}\ 2O_2 + 2e^-$) and the resulting O_2 created pressure on the sensing electrode. It resulted in negative linearity with ΔV. The sensing mechanism is well elucidated based on the mixed potential model and substantiated using polarization curve measurements. A schematic representation of the device is shown in Fig. 13(b).[149] The fabricated sensor also exhibited good reproducibility and selectivity toward NO_2 and these attractive sensing characteristics indicate this NO_2 sensor using $CoTiO_3$ to be a promising detection device for automotive exhaust.

The ($LaFeO_3$ (LFO) hollow micro spindles derived from a metal–organic framework, with a longitudinal dimension of 5 μm by a self-template chemical process were used with the Ag reference electrode for NO_2 gas sensing at a much lower operating temperature of 155 °C. A high limit of detection of 5 ppm was observed for NO_2 gas and the device was cost-effective. According to the reaction mechanism, when the LFO layer was exposed to NO_2 gas it resulted in the direct capture of electrons and the formation of surface-adsorbed nitrite species, $NO_2^-{}_{(ads)} \rightarrow NO_{(gas)} + O^-{}_{(ads)}$, through catalytic decomposition. A schematic representation of the device is given in Fig. 13(c).[150]

The same $LaFeO_3$ perovskite electrode was decorated with PdO NPs for enhancing the sensitivity, stability, and selectivity of the gas sensor, and this strategy was found to be suitable for application to other sensor devices as well. The oxidation process initiated due to the transfer of electrons from the sensor electrode allowed the NO_2 gas to react, resulting in the formation of O^{2-}, which in turn reacted with the reference electrode to form O_2 (reaction to SE side: $NO_2 + 2e^- \rightarrow NO + O^{2-}$ and reaction to RE side: $O^2–2e^- \rightarrow 1/2O_2$).[151]

A Cu-doped $NaBiTiO_3$ (NBTC) perovskite was also developed as an amperometric type NO_2 sensor. The study reported the sensitive response of NBTC (0.15 to 500 ppm) towards NO_2 gas sensing at the current value of 2.25 μA at 500 °C. Thus, they proposed that the sensitivity and stability of the developed device could be applied in real-time applications, mostly in automotive exhaust.[152] Table 3 gives the comparison of detection limits of various perovskite materials used for gas sensing.

6. Conclusions and perspectives

Researchers have been successfully exploiting the ability of perovskites to transmute external stimulants into highly optical and electrical signals. Optical sensing is mainly a fluorescence-based process, and it occurs *via* FRET, electron transfer, or cation exchange. ABX_3-type perovskites appear to be promising materials for optical sensing for metal ions such as Cu^{2+}, Hg^{2+}, Pb^{2+} Co^{2+}, *etc*. but they lack practical application due to their moisture sensitivity. As mentioned, regardless of the difficulty in achieving the fabrication of these perovskite materials as sensing probes, enhancing their stability is a very challenging task. Over the past few years, some of the methods, including ligand exchange, doping, the formation of heterostructures, and hybridization with porous membranes,

have been attempted to improve the stability of perovskites but with little success for sensing applications. Contemplating the fact that these perovskites are affected by external factors such as temperature, humidity, gases, and solvents, designing these sensors in the real intricate environment is important. The intrinsic toxicity of Pb is another serious issue that must be considered. It is well known that the lone pair of electrons ($6s^2$) in Pb species, which align with halides, is responsible for the high fluorescence of Pb that gives way for sensing. Although one can find may reports on the replacement of Pb by Ge, Sn, Bi, and Cu, their application for sensing activity seems limited. Double perovskites, wherein Pb cations are replaced by two other cations, namely, Ag, Bi, In and Sb, have shown good photovoltaic properties and also stability, and thus can be explored for such sensing applications. However, this study will have an upper hand (reach another level) over a wide range of practical applications if water-stable PNCs are discovered.

The perovskite-based electrode materials using the ABO_3-type structure have been proved for sensing by different electrochemical approaches mostly with GCE and SPCE using cyclic voltammetry and square wave voltammetry techniques. These sensors showed good detection limits, repeatability, reproducibility, and high selectivity towards the sensing of various environmental pollutants and drugs. With low cost, prompt detection, trace-level LODs, wide linear range, good sensitivity, reproducibility, excellent stability, and accuracy, these sensors could potentially be utilized for screening various environmental pollutants and drugs in remote areas. Therefore, these kinds of sensing work conducted on inorganic perovskite oxide-based materials offer promises to design probes for electrochemical detections in real-time conditions. There is, however, scope to enhance the sensitivity levels with the fine-tuning of surface area, crystal size, and structure, which is at present scarcely explored. Applications in the areas of the sensing of emerging contaminants and PPCPs (Pharma and Personal Care Products) using these perovskites seems very promising for future studies.

With regard to gas sensing, devices based on perovskite materials have been successfully fabricated and efficiently used to sense some of the essential gases such as N_2, H_2S, H_2, NO_2, NH_3 and O_2 *via* electron transfer and adsorption. Target gas molecules feasibly adsorb onto trap states and defects of perovskites, and sometimes also intercalate into their lattices resulting in intermediate complexes that can be reversed thus facilitating sensing ability. Compared to other gas sensors, most of these perovskite gas sensors can be operated at room temperature. Organometallic halide perovskites, being good semiconductors and showing response to conductivity on interaction with target gases, can be practically applied in vacuum or inert conditions to detect gas molecules. The changes in the resistance of these semiconducting perovskites on interaction with gases such as O_2, CO and NH_3 open up vast possibilities for the development of more sensitive sensors. Protected surfaces with considerably improved stability have been attempted for sensing gases in real-time. There are studies wherein perovskite sensors are practically applied, as in ozone sensors that can detect very low concentrations, up to ppb levels. The formation of perovskite composites with stable materials, and incorporating them into porous structures and membranes could also be new areas for exploring them as stable perovskite sensors for gas detection. The simultaneous detection of more than one gas at a time will be another significant development in the years to come.

Conflicts of interest

There are no conflicts to declare.

Acknowledgements

The authors gratefully acknowledge the SERB Department of Science and Technology, Govt. of India for the funding support (Project No. CRG/2018/000942) to carry out this work.

References

1 J. A. Garcia-Mesa and R. Mateos, Direct Automatic Determination of Bitterness and Total Phenolic Compounds in Virgin Olive Oil Using a pH-Based Flow-Injection Analysis System, *J. Agric. Food Chem.*, 2007, **55**(10), 3863–3868, DOI: 10.1021/jf070235v.

2 A. Asan and I. Isildak, Determination of major phenolic compounds in water by reversed-phase liquid chromatography after pre-column derivatization with benzoyl chloride, *J. Chromatogr., A*, 2003, **988**(1), 145–149, DOI: 10.1016/s0021-9673(02)02056-3.

3 T. C. Canevari, P. A. Raymundo-Pereira, R. Landers and S. A. S. Machado, Direct Synthesis of Ag Nanoparticles Incorporated on a Mesoporous Hybrid Material as a Sensitive Sensor for the Simultaneous Determination of Dihydroxybenzenes Isomers, *Eur. J. Inorg. Chem.*, 2013, **2013**(33), 5746–5754, DOI: 10.1002/ejic.201300879.

4 G. H. Ribeiro, L. M. Vilarinho, T. d. S. Ramos, A. L. Bogado and L. R. Dinelli, Electrochemical behavior of hydroquinone and catechol at glassy carbon electrode modified by electropolymerization of tetraruthenated oxovanadium porphyrin, *Electrochim. Acta*, 2015, **176**, 394–401, DOI: 10.1016/j.electacta.2015.06.139.

5 P. Ramakrishnan and K. Rangiah, A UHPLC-MS/SRM method for analysis of phenolics from Camellia sinensis leaves from Nilgiri hills, *Anal. Methods*, 2016, **8**(45), 8033–8041, DOI: 10.1039/c6ay02329k.

6 D. Xiong and H. Li, Colorimetric detection of pesticides based on calixarene modified silver nanoparticles in water, *Nanotechnology*, 2008, **19**(46), 465502, DOI: 10.1088/0957-4484/19/46/465502.

7 D. Maity and T. Govindaraju, Highly Selective Colorimetric Chemosensor for Co2+, *Inorg. Chem.*, 2011, **50**(22), 11282–11284, DOI: 10.1021/ic2015447.

8 A. Hulanicki, S. Glab and F. Ingman, Chemical sensors: definitions and classification, *Pure Appl. Chem.*, 1991, **63**(9), 1247–1250, DOI: 10.1351/pac199163091247.
9 M. J. Comstock and M. J. Comstock, *Fluorescent Chemosensors for Ion and Molecule Recognition, Copyright, 1993 Advisory Board, Foreword*, 1993, pp. i–vi. DOI: 10.1021/bk-1993-0538.
10 J. Janata, *Principles of Chemical Sensors*, 2009. DOI: 10.1007/b136378.
11 L. Basabe-Desmonts, D. N. Reinhoudt and M. Crego-Calama, Design of fluorescent materials for chemical sensing, *Chem. Soc. Rev.*, 2007, **36**(6), 993, DOI: 10.1039/b609548h.
12 T. S. Snowden and E. V. Anslyn, Anion recognition: synthetic receptors for anions and their application in sensors, *Curr. Opin. Chem. Biol.*, 1999, **3**(6), 740–746, DOI: 10.1016/s1367-5931(99)00034-4.
13 L. Fabbrizzi, M. Licchelli, F. Mancin, M. Pizzeghello, G. Rabaioli, A. Taglietti, P. Tecilla and U. Tonellato, Fluorescence Sensing of Ionic Analytes in Water: From Transition Metal Ions to Vitamin B13, *Chem. – Eur. J.*, 2002, **8**(1), 94–101, DOI: 10.1002/1521-3765(20020104)8:1<94::aid-chem94>3.0.co;2-l.
14 L. Järup, Hazards of heavy metal contamination, *Br. Med. Bull.*, 2003, **68**(1), 167–182, DOI: 10.1093/bmb/ldg032.
15 S. L. Wiskur, H. Ait-Haddou, J. J. Lavigne and E. V. Anslyn, Teaching Old Indicators New Tricks, *Acc. Chem. Res.*, 2001, **34**(12), 963–972, DOI: 10.1021/ar9600796.
16 U. Resch-Genger, M. Grabolle, S. Cavaliere-Jaricot, R. Nitschke and T. Nann, Quantum dots versus organic dyes as fluorescent labels, *Nat. Methods*, 2008, **5**(9), 763–775, DOI: 10.1038/nmeth..
17 Y. H. Lau, P. J. Rutledge, M. Watkinson and M. H. Todd, Chemical sensors that incorporate click-derived triazoles, *Chem. Soc. Rev.*, 2011, **40**(5), 2848, DOI: 10.1039/c0cs00143k.
18 D.-L. Ma, V. P.-Y. Ma, D. S.-H. Chan, K.-H. Leung, H.-Z. He and C.-H. Leung, Recent advances in luminescent heavy metal complexes for sensing, *Coord. Chem. Rev.*, 2012, **256**(23–24), 3087–3113, DOI: 10.1016/j.ccr.2012.07.005.
19 C. Li and G. Shi, Carbon nanotube-based fluorescence sensors, *J. Photochem. Photobiol., C*, 2014, **19**, 20–34, DOI: 10.1016/j.jphotochemrev.2013.10.005.
20 C. J. Chang, T. Gunnlaugsson and T. D. James, Sensor targets, *Chem. Soc. Rev.*, 2015, **44**(13), 4176–4178, DOI: 10.1039/c5cs90058a.
21 C. J. Chang, T. Gunnlaugsson and T. D. James, Imaging agents, *Chem. Soc. Rev.*, 2015, **44**(14), 4484–4486, DOI: 10.1039/c5cs90065d.
22 S. M. Ng, M. Koneswaran and R. Narayanaswamy, A review on fluorescent inorganic nanoparticles for optical sensing applications, *RSC Adv.*, 2016, **6**, 21624–21661.
23 S. M. Ng, M. Koneswaran and R. Narayanaswamy, A review on fluorescent inorganic nanoparticles for optical sensing applications, *RSC Adv.*, 2016, **6**(26), 21624–21661, DOI: 10.1039/c5ra24987b.
24 V. V. Halali, M. Saxena, H. R. Chandan, A. A. Ojha and R. G. Balakrishna, Paper based field deployable sensor for naked eye monitoring of copper(II) ions elucidation of binding mechanism by DFT studies, *Spectrochim. Acta, Part A*, 2019, 117291, DOI: 10.1016/j.saa.2019.117291.
25 V. H. Vishaka, S. Manav, R. Geetha Balakrishna, L. Sachin and J. Shilpee, Remarkably selective biocompatible turn-on fluorescent probe for detection of Fe3+in human blood samples and cells, *RSC Adv.*, 2019, **9**(47), 27439–27448, DOI: 10.1039/C9RA05256A.
26 J. Xing, X. F. Liu, Q. Zhang, S. T. Ha, Y. W. Yuan, C. Shen, T. C. Sum and Q. Xiong, Vapor Phase Synthesis of Organometal Halide Perovskite Nanowires for Tunable Room-Temperature Nanolasers, *Nano Lett.*, 2015, **15**(7), 4571–4577, DOI: 10.1021/acs.nanolett.5b01166.
27 J. Dai, H. Zheng, C. Zhu, J. Lu and C. Xu, Comparative investigation on temperature-dependent photoluminescence of CH3NH3PbBr3 and CH(NH2)2PbBr3 microstructures, *J. Mater. Chem. C*, 2016, **4**(20), 4408–4413, DOI: 10.1039/c6tc00563b.
28 G. Yang, Q. Fan, B. Chen, Q. Zhou and H. Zhong, Reprecipitation synthesis of luminescent CH3NH3PbBr3/NaNO3 nanocomposites with enhanced stability, *J. Mater. Chem. C*, 2016, **4**(48), 11387–11391, DOI: 10.1039/c6tc04069a.
29 H. Huang, M. Liu, J. Li, L. Luo, J. Zhao, Z. Luo, X. Wang, Z. Ye, H. He and J. Zeng, Atomically thin cesium lead bromide perovskite quantum wires with high luminescence, *Nanoscale*, 2017, **9**(1), 104–108, DOI: 10.1039/c6nr08250e.
30 D. Priante, I. Dursun, M. S. Alias, D. Shi, V. A. Melnikov, T. K. Ng, O. F. Mohammed, O. M. Bakr, and B. S. Ooi, The recombination mechanisms leading to amplified spontaneous emission at the true-green wavelength in CH3NH3PbBr3 perovskites, *Appl. Phys. Lett.*, 2015, **106**(8), 081902, DOI: 10.1063/1.4913463.
31 G. Grancini, V. D'Innocenzo, E. R. Dohner, N. Martino, A. R. Srimath Kandada, E. Mosconi, F. De Angelis, H. I. Karunadasa, E. T. Hoke and A. Petrozza, CH3NH3PbI3 perovskite single crystals: surface photophysics and their interaction with the environment, *Chem. Sci.*, 2015, **6**(12), 7305–7310, DOI: 10.1039/c5sc02542g.
32 N. A. Manshor, Q. Wali, K. K. Wong, S. K. Muzakir, A. Fakharuddin, L. Schmidt-Mende and R. Jose, Humidity versus photo-stability of metal halide perovskite films in a polymer matrix, *Phys. Chem. Chem. Phys.*, 2016, **18**(31), 21629–21639, DOI: 10.1039/c6cp03600g.
33 S. Pathak, A. Sepe, A. Sadhanala, F. Deschler, A. Haghighirad, N. Sakai, K. C. Goedel, S. D. Stranks, N. Noel, M. Price, S. Hüttner, N. A. Hawkins, R. H. Friend, U. Steiner, and H. J. Snaith, Atmospheric Influence upon Crystallization and Electronic Disorder and Its Impact on the Photophysical Properties of Organic–Inorganic Perovskite Solar Cells, *ACS Nano*, 2015, **9**(3), 2311–2320, DOI: 10.1021/nn506465n.

34 Z. Zhu, Q. Sun, Z. Zhang, J. Dai, G. Xing, S. Li, X. Huang and W. Huang, Metal halide perovskites: stability and sensing-ability, *J. Mater. Chem. C*, 2018, **6**(38), 10121–10137, DOI: 10.1039/C8TC03164A.

35 P. Wu, T. Zhao, S. Wang and X. Hou, Semicondutor quantum dots-based metal ion probes, *Nanoscale*, 2014, **6**(1), 43–64, DOI: 10.1039/c3nr04628a.

36 D. T. Quang and J. S. Kim, Fluoro- and Chromogenic Chemodosimeters for Heavy Metal Ion Detection in Solution and Biospecimens, *Chem. Rev.*, 2010, **110**(10), 6280–6301, DOI: 10.1021/cr100154p.

37 D. W. Domaille, E. L. Que and C. J. Chang, Synthetic fluorescent sensors for studying the cell biology of metals, *Nat. Chem. Biol.*, 2008, **4**(3), 168–175, DOI: 10.1038/nchembio.69.

38 X. Chen, T. Pradhan, F. Wang, J. S. Kim and J. Yoon, Fluorescent Chemosensors Based on Spiroring-Opening of Xanthenes and Related Derivatives, *Chem. Rev.*, 2011, **112**(3), 1910–1956, DOI: 10.1021/cr200201z.

39 H. N. Kim, W. X. Ren, J. S. Kim and J. Yoon, Fluorescent and colorimetric sensors for detection of lead, cadmium, and mercury ions, *Chem. Soc. Rev.*, 2012, **41**(8), 3210–3244, DOI: 10.1039/c1cs15245a.

40 Z. Xu, J. Yoon and D. R. Spring, Fluorescent chemosensors for Zn2+, *Chem. Soc. Rev.*, 2010, **39**(6), 1996, DOI: 10.1039/b916287a.

41 *Principles of Fluorescence Spectroscopy*, ed. J. R. Lakowicz, 2006. DOI: 10.1007/978-0-387-46312-4.

42 W. T. Mason, *Fluorescent and luminescent probes for biological activity: a practical guide to technology for quantitative real-time analysis*, Elsevier, 1999.

43 I. Borriello, G. Cantele and D. Ninno, Ab initio investigation of hybrid organic-inorganic perovskites based on tin halides, *Phys. Rev. B: Condens. Matter Mater. Phys*, 2009, **77**(23), 235214, DOI: 10.1103/PhysRevB.77.235214.

44 L. Protesescu, S. Yakunin, M. I. Bodnarchuk, F. Krieg, R. Caputo, C. H. Hendon, R. X. Yang, A. Walsh and M. V. Kovalenko, Nanocrystals of Cesium Lead Halide Perovskites (CsPbX3, X=Cl, Br, and I): Novel Optoelectronic Materials Showing Bright Emission with Wide Color Gamut, *Nano Lett.*, 2015, **15**(6), 3692–3696, DOI: 10.1021/nl5048779.

45 F. Zhang, H. Zhong, C. Chen, X. G. Wu, X. Hu, H. Huang, J. Han, B. Zou and Y. Dong, Brightly Luminescent and Color-Tunable Colloidal CH3NH3PbX3 (X=Br, I, Cl) Quantum Dots: Potential Alternatives for Display Technology, *ACS Nano*, 2015, **9**(4), 4533–4542, DOI: 10.1021/acsnano.5b01154.

46 S. Colella, M. Mazzeo, A. Rizzo, G. Gigli and A. Listorti, The Bright Side of Perovskites, *J. Phys. Chem. Lett.*, 2016, **7**(21), 4322–4334, DOI: 10.1021/acs.jpclett.6b01799.

47 H. Huang, M. I. Bodnarchuk, S. V. Kershaw, M. V. Kovalenko and A. L. Rogach, Lead Halide Perovskite Nanocrystals in the Research Spotlight: Stability and Defect Tolerance, *ACS Energy Lett.*, 2017, **2**(9), 2071–2083, DOI: 10.1021/acsenergylett.7b00547.

48 H. Zhou, Q. Chen, G. Li, S. Luo, T. Song, H. S. Duan, Z. Hong, J. You, Y. Liu and Y. Yang, Interface engineering of highly efficient perovskite solar cells, *Science*, 2014, **345**(6196), 542–546, DOI: 10.1126/science.1254050.

49 B. L. Watson, N. Rolston, A. D. Printz and R. H. Dauskardt, Scaffold-reinforced perovskite compound solar cells, *Energy Environ. Sci.*, 2017, **10**(12), 2500–2508, DOI: 10.1039/c7ee02185b.

50 N. J. Jeon, J. H. Noh, Y. C. Kim, W. S. Yang, S. Ryu and S. I. Seok, Solvent engineering for high-performance inorganic–organic hybrid perovskite solar cells, *Nat. Mater.*, 2014, **13**(9), 897–903, DOI: 10.1038/nmat4014.

51 W. Wang, Y. He and L. Qi, High-efficiency colorful perovskite solar cells using TiO_2 nanobowl arrays as a structured electron transport layer, *Sci. China Mater.*, 2019, **63**(1), 35–46, DOI: 10.1007/s40843-019-9452-1.

52 L. Dou, Y. M. Yang, J. You, Z. Hong, W. H. Chang, G. Li and Y. Yang, Solution-processed hybrid perovskite photodetectors with high detectivity, *Nat. Commun.*, 2014, **5**, 5404, DOI: 10.1038/ncomms6404.

53 M. I. Saidaminov, V. Adinolfi, R. Comin, A. L. Abdelhady, W. Peng, I. Dursun, M. Yuan, S. Hoogland, E. H. Sargent and O. M. Bakr, Planar-integrated single-crystalline perovskite photodetectors, *Nat. Commun.*, 2015, **6**, 8724, DOI: 10.1038/ncomms9724.

54 J. Zhou, Y. Chu and J. Huang, Photodetectors Based on Two-Dimensional Layer-Structured Hybrid Lead Iodide Perovskite Semiconductors, *ACS Appl. Mater. Interfaces*, 2016, **8**(39), 25660–25666, DOI: 10.1021/acsami.6b09489.

55 Q. Zhang, R. Su, X. Liu, J. Xing, T. C. Sum and Q. Xiong, High-Quality Whispering-Gallery-Mode Lasing from Cesium Lead Halide Perovskite Nanoplatelets, *Adv. Funct. Mater.*, 2016, **26**(34), 6238–6245, DOI: 10.1002/adfm.201601690.

56 P. Brenner, T. Glöckler, D. R. Delgado, T. Abzieher, M. Jakoby, B. S. Richards, U. W. Paetzold, I. A. Howard and U. Lemmer, Triple cation mixed-halide perovskites for tunable lasers, *Opt. Mater. Express*/, 2017, **7**(11), 4082, DOI: 10.1364/ome.7.004082.

57 J. Song, J. Li, X. Li, L. Xu, Y. Dong and H. Zeng, Quantum Dot Light-Emitting Diodes Based on Inorganic Perovskite Cesium Lead Halides (CsPbX3), *Adv. Mater.*, 2015, **27**(44), 7162–7167, DOI: 10.1002/adma.201502567.

58 J. Byun, H. Cho, C. Wolf, M. Jang, A. Sadhanala, R. H. Friend, H. Yang and T. W. Lee, Efficient Visible Quasi-2D Perovskite Light-Emitting Diodes, *Adv. Mater.*, 2016, **28**(34), 7515–7520, DOI: 10.1002/adma.201601369.

59 S. A. Veldhuis, P. P. Boix, N. Yantara, M. Li, T. C. Sum, N. Mathews and S. G. Mhaisalkar, Perovskite Materials for Light-Emitting Diodes and Lasers, *Adv. Mater.*, 2016, **28**(32), 6804–6834, DOI: 10.1002/adma.201600669.

60 L. Meng, E. P. Yao, Z. Hong, H. Chen, P. Sun, Z. Yang, G. Li and Y. Yang, Pure Formamidinium-Based Perovskite Light-Emitting Diodes with High Efficiency and Low Driving Voltage, *Adv. Mater.*, 2016, **29**(4), 1603826, DOI: 10.1002/adma.201603826.

61 Z. Xiao, R. A. Kerner, L. Zhao, N. L. Tran, K. M. Lee, T. W. Koh, G. D. Scholes and B. P. Rand, Efficient perovskite light-emitting diodes featuring nanometre-sized crystallites, *Nat. Photonics*, 2017, **11**(2), 108–115, DOI: 10.1038/nphoton.2016.269.

62 G. Hodes, Perovskite-Based Solar Cells, *Science*, 2013, **342**(6156), 317–318, DOI: 10.1126/science.1245473.

63 S. D Stranks, G. E. Eperon, G. Grancini, C. Menelaou, M. J. P. Alcocer, T. Leijtens, L. M. Herz, A. Petrozza and H. J. Snaith, Electron-Hole Diffusion Lengths Exceeding 1 Micrometer in an Organometal Trihalide Perovskite Absorber, *Science*, 2013, **342**(6156), 341–344, DOI: 10.1126/science.1243982.

64 Z. K. Tan, R. S. Moghaddam, M. L. Lai, P. Docampo, R. Higler, F. Deschler, M. Price, A. Sadhanala, L. M. Pazos, D. Credgington, F. Hanusch, T. Bein, H. J. Snaith and R. H. Friend, Bright light-emitting diodes based on organometal halide perovskite, *Nat. Nanotechnol.*, 2014, **9**(9), 687–692, DOI: 10.1038/nnano.2014.149.

65 D. Shi, V. Adinolfi, R. Comin, M. Yuan, E. Alarousu, A. Buin, Y. Chen, S. Hoogland, A. Rothenberger, K. Katsiev, Y. Losovyj, X. Zhang, P. A. Dowben, O. F. Mohammed, E. H. Sargent and O. M. Bakr, Low trap-state density and long carrier diffusion in organolead trihalide perovskite single crystals, *Science*, 2015, **347**(6221), 519–522, DOI: 10.1126/science.aaa2725.

66 X. Li, Y. Wu, S. Zhang, B. Cai, Y. Gu, J. Song and H. Zeng, CsPbX3Quantum Dots for Lighting and Displays: Room-Temperature Synthesis, Photoluminescence Superiorities, Underlying Origins and White Light-Emitting Diodes, *Adv. Funct. Mater.*, 2016, **26**(15), 2435–2445, DOI: 10.1002/adfm.201600109.

67 G. R. Yettapu, D. Talukdar, S. Sarkar, A. Swarnkar, A. Nag, P. Ghosh and P. Mandal, Terahertz Conductivity within Colloidal CsPbBr3 Perovskite Nanocrystals: Remarkably High Carrier Mobilities and Large Diffusion Lengths, *Nano Lett.*, 2016, **16**(8), 4838–4848, DOI: 10.1021/acs.nanolett.6b01168.

68 Y. Ling, Z. Yuan, Y. Tian, X. Wang, J. C. Wang, Y. Xin, K. Hanson, B. Ma and H. Gao, Bright Light-Emitting Diodes Based on Organometal Halide Perovskite Nanoplatelets, *Adv. Mater.*, 2015, **28**(2), 305–311, DOI: 10.1002/adma.201503954.

69 N. Dhenadhayalan, H.-L. Lee, K. Yadav, K.-C. Lin, Y.-T. Lin and A. H. H. Chang, Silicon Quantum Dot-Based Fluorescence Turn-On Metal Ion Sensors in Live Cells, *ACS Appl. Mater. Interfaces*, 2016, **8**(36), 23953–23962, DOI: 10.1021/acsami.6b07789.

70 K. P. Carter, A. M. Young and A. E. Palmer, Fluorescent Sensors for Measuring Metal Ions in Living Systems, *Chem. Rev.*, 2014, **114**(8), 4564–4601, DOI: 10.1021/cr400546e.

71 S. Chowdhury, B. Rooj, A. Dutta and U. Mandal, Review on Recent Advances in Metal Ions Sensing Using Different Fluorescent Probes, *J. Fluoresc.*, 2018, **28**(4), 999–1021, DOI: 10.1007/s10895-018-2263-y.

72 H. R. Chandan, M. Venkataramana, M. D. Kurkuri and R. Geetha Balakrishna, Simple quantum dot bioprobe/label for sensitive detection of Staphylococcus aureus TNase, *Sens. Actuators, B*, 2016, **222**, 1201–1208, DOI: 10.1016/j.snb.2015.07.121.

73 H. R. C, J. D. Schiffman and R. G. Balakrishna, Quantum dots as fluorescent probes: Synthesis, surface chemistry, energy transfer mechanisms, and applications, *Sens. Actuators, B*, 2018, **258**, 1191–1214, DOI: 10.1016/j.snb.2017.11.189.

74 H. R. Chandan, M. Ira Gowda and R. G. Balakrishna, An "OFF–ON" quantum dot–graphene oxide bioprobe for sensitive detection of micrococcal nuclease of Staphylococcus aureus, *Analyst*, 2019, **144**(13), 3999–4005, DOI: 10.1039/C8AN02116C.

75 H. R. Chandan, V. Saravanan, P. Ranjith Krishna and R. Geetha Balakrishna, Synergistic effect of binary ligands on nucleation and growth/size effect of nanocrystals: Studies on reusability of the solvent, *J. Mater. Res.*, 2014, **29**(14), 1556–1564, DOI: 10.1557/jmr.2014.180.

76 L. P. D'Souza, V. Amoli, H. R. Chandan, A. K. Sinha, P. Ranjith Krishna and G. R. Balakrishna, Atomic force microscopic study of nanoscale interaction between N719 dye and CdSe quantum dot in hybrid solar cells and their enhanced open circuit potential, *Sol. Energy*, 2015, **116**, 25–36, DOI: 10.1016/j.solener.2015.03.036.

77 J. J. Li, Y. A. Wang, W. Guo, J. C. Keay, T. D. Mishima, M. B. Johnson and X. Peng, Large-Scale Synthesis of Nearly Monodisperse CdSe/CdS Core/Shell Nanocrystals Using Air-Stable Reagents via Successive Ion Layer Adsorption and Reaction, *J. Am. Chem. Soc.*, 2003, **125**(41), 12567–12575, DOI: 10.1021/ja0363563.

78 M. Aamir, M. Sher, M. A. Malik, J. Akhtar and N. Revaprasadu, A chemodosimetric approach for the selective detection of Pb2+ions using a cesium based perovskite, *New J. Chem.*, 2016, **40**(11), 9719–9724, DOI: 10.1039/c6nj01783e.

79 L.-Q. Lu, T. Tan, X.-K. Tian, Y. Li and P. Deng, Visual and sensitive fluorescent sensing for ultratrace mercury ions by perovskite quantum dots, *Anal. Chim. Acta*, 2017, **986**, 109–114, DOI: 10.1016/j.aca.2017.07.014.

80 B. Park, S. M. Kang, G. W. Lee, C. H. Kwak, M. Rethinasabapathy and Y. S. Huh, Fabrication of CsPbBr3 Perovskite Quantum Dots/Cellulose- based Colorimetric Sensor: Dual-Responsive On-site Detection of Chloride and Iodide Ions, *Ind. Eng. Chem. Res.*, 2020, **59**(2), 793–801, DOI: 10.1021/acs.iecr.9b05946.

81 L. Bian, Y. Li, J. Li, J. Nie, F. Dong, M. Song, L. Wang, H. Dong, H. Li, X. Nie, X. Zhang, X. Li and L. Xie, Photovoltage response of (XZn)Fe 2 O 4 -BiFeO 3 (X=Mg, Mn or Ni) interfaces for highly selective Cr 3+, Cd 2+, Co 2+ and Pb 2+ ions detection, *J. Hazard. Mater.*, 2017, **336**, 174–187, DOI: 10.1016/j.jhazmat.2017.04.071.

82 X. Sheng, Y. Liu, Y. Wang, Y. Li, X. Wang, X. Wang, Z. Dai, J. Bao and X. Xu, Cesium Lead Halide Perovskite Quantum Dots as a Photoluminescence Probe for Metal

Ions, *Adv. Mater.*, 2017, **29**(37), 1700150, DOI: 10.1002/adma.201700150.

83 Y. Liu, X. Tang, T. Zhu, M. Deng, I. P. Ikechukwu, W. Huang, G. Yin, Y. Bai, D. Qu, X. Huang and F. Qiu, All-inorganic CsPbBr3 perovskite quantum dots as a photoluminescent probe for ultrasensitive Cu2+ detection, *J. Mater. Chem. C*, 2018, **6**(17), 4793–4799, DOI: 10.1039/c8tc00249e.

84 N. Ding, D. Zhou, G. Pan, W. Xu, X. Chen, D. Li, X. Zhang, J. Zhu, Y. Ji and H. Song, Europium-doped lead-free $Cs_3Bi_2Br_9$ perovskite quantum dots and ultrasensitive Cu^{2+} detection, *ACS Sustainable Chem. Eng.*, 2019, **7**(9), 8397–8404, DOI: 10.1021/acssuschemeng.9b00038.

85 S. Huang, M. Guo, J. Tan, Y. Geng, J. Wu, Y. Tang, C. Su, C. C. Lin and Y. Liang, Novel fluorescence sensor based on all-inorganic perovskite quantum dots coated with molecularly imprinted polymers for highly selective and sensitive detection of omethoate, *ACS Appl. Mater. Interfaces*, 2018, **10**(45), 39056–39063, DOI: 10.1021/acsami.8b14472.

86 L. Tan, M. Guo, J. Tan, Y. Geng, S. Huang, Y. Tang, C. Su, C. Lin and Y. Liang, Development of high-luminescence perovskite quantum dots coated with molecularly imprinted polymers for pesticide detection by slowly hydrolysing the organosilicon monomers in situ, *Sens. Actuators, B*, 2019, **291**, 226–234, DOI: 10.1016/j.snb.2019.04.079.

87 Y. Huang, F. Yan, J. Xu, Y. Bian, R. Zhang, J. Wang and X. Zhou, The FRET performance and aggregation-induced emission of two-dimensional organic-inorganic perovskite, and its application to the determination of Hg(II), *Microchim. Acta*, 2017, **184**(9), 3513–3519, DOI: 10.1007/s00604-017-2360-7.

88 Y. Wang, Y. Zhu, J. Huang, J. Cai, J. Zhu, X. Yang, J. Shen and C. Li, Perovskite quantum dots encapsulated in electrospun fiber membranes as multifunctional supersensitive sensors for biomolecules, metal ions and pH, *Nanoscale Horiz.*, 2017, **2**(4), 225–232, DOI: 10.1039/c7nh00057j.

89 J. Xing, X. F. Liu, Q. Zhang, S. T. Ha, Y. W. Yuan, C. Shen, T. C. Sum and Q. Xiong, Vapor Phase Synthesis of Organometal Halide Perovskite Nanowires for Tunable Room-Temperature Nanolasers, *Nano Lett.*, 2015, **15**(7), 4571–4577, DOI: 10.1021/acs.nanolett.5b01166.

90 J. Yang, B. D. Siempelkamp, D. Liu and T. L. Kelly, Investigation of CH3NH3PbI3 Degradation Rates and Mechanisms in Controlled Humidity Environments Using in Situ Techniques, *ACS Nano*, 2015, **9**(2), 1955–1963, DOI: 10.1021/nn506864k.

91 L. Hu, G. Shao, T. Jiang, D. Li, X. Lv, H. Wang, X. Liu, H. Song, J. Tang and H. Liu, Investigation of the Interaction between Perovskite Films with Moisture via in Situ Electrical Resistance Measurement, *ACS Appl. Mater. Interfaces*, 2015, **7**(45), 25113–25120, DOI: 10.1021/acsami.5b06268.

92 Y. Tian, A. Merdasa, E. Unger, M. Abdellah, K. Zheng, S. McKibbin, A. Mikkelsen, T. Pullerits, A. Yartsev, V. Sundström and I. G. Scheblykin, Enhanced Organo-Metal Halide Perovskite Photoluminescence from Nanosized Defect-Free Crystallites and Emitting Sites, *J. Phys. Chem. Lett.*, 2015, **6**(20), 4171–4177, DOI: 10.1021/acs.jpclett.5b02033.

93 G. Kieslich, S. Sun and A. K. Cheetham, Solid-state principles applied to organic–inorganic perovskites: new tricks for an old dog, *Chem. Sci.*, 2014, **5**(12), 4712–4715, DOI: 10.1039/c4sc02211d.

94 C. C. Stoumpos and M. G. Kanatzidis, The Renaissance of Halide Perovskites and Their Evolution as Emerging Semiconductors, *Acc. Chem. Res.*, 2015, **48**(10), 2791–2802, DOI: 10.1021/acs.accounts.5b00229.

95 Z. Li, M. Yang, J.-S. Park, S.-H. Wei, J. J. Berry and K. Zhu, Stabilizing Perovskite Structures by Tuning Tolerance Factor: Formation of Formamidinium and Cesium Lead Iodide Solid-State Alloys, *Chem. Mater.*, 2015, **28**(1), 284–292, DOI: 10.1021/acs.chemmater.5b04107.

96 N. Ahn, D.-Y. Son, I.-H. Jang, S. M. Kang, M. Choi and N.-G. Park, Highly Reproducible Perovskite Solar Cells with Average Efficiency of 18.3% and Best Efficiency of 19.7% Fabricated via Lewis Base Adduct of Lead(II) Iodide, *J. Am. Chem. Soc.*, 2015, **137**(27), 8696–8699, DOI: 10.1021/jacs.5b04930.

97 J.-W. Lee, S.-H. Bae, Y.-T. Hsieh, N. De Marco, M. Wang, P. Sun and Y. Yang, A Bifunctional Lewis Base Additive for Microscopic Homogeneity in Perovskite Solar Cells, *Chem*, 2017, **3**(2), 290–302, DOI: 10.1016/j.chempr.2017.05.020.

98 X. Li, M. Ibrahim Dar, C. Yi, J. Luo, M. Tschumi, S. M. Zakeeruddin, M. K. Nazeeruddin, H. Han and M. Grätzel, Improved performance and stability of perovskite solar cells by crystal crosslinking with alkylphosphonic acid ω-ammonium chlorides, *Nat. Chem.*, 2015, **7**(9), 703–711, DOI: 10.1038/nchem.2324.

99 D. Shen, A. Pang, Y. Li, J. Dou and M. Wei, Metal–organic frameworks at interfaces of hybrid perovskite solar cells for enhanced photovoltaic properties, *Chem. Commun.*, 2018, **54**(10), 1253–1256, DOI: 10.1039/c7cc09452c.

100 S. Mollick, T. N. Mandal, A. Jana, S. Fajal, A. V. Desai and S. K. Ghosh, Ultrastable luminescent hybrid bromide perovskite@mof nanocomposites for the degradation of organic pollutants in water, *ACS Appl. Nano Mater.*, 2019, **2**(3), 1333–1340, DOI: 10.1021/acsanm.8b02214.

101 Y. Zhao, J. Wei, H. Li, Y. Yan, W. Zhou, D. Yu and Q. Zhao, A polymer scaffold for self-healing perovskite solar cells, *Nat. Commun.*, 2016, **7**, 10228, DOI: 10.1038/ncomms10228.

102 Y. Guo, K. Shoyama, W. Sato and E. Nakamura, Polymer Stabilization of Lead(II) Perovskite Cubic Nanocrystals for Semitransparent Solar Cells, *Adv. Energy Mater.*, 2016, **6**(6), 1502317, DOI: 10.1002/aenm.201502317.

103 L. Zuo, H. Guo, D. W. deQuilettes, S. Jariwala, N. De Marco, S. Dong, R. DeBlock, D. S. Ginger, B. Dunn, M. Wang and Y. Yang, Polymer-modified halide perovskite films for efficient and stable planar heterojunction solar cells, *Sci. Adv.*, 2017, **3**(8), e1700106, DOI: 10.1126/sciadv.1700106.

104 L. Gomez, C. de Weerd, J. L. Hueso and T. Gregorkiewicz, Color-stable water-dispersed cesium lead halide perovskite nanocrystals, *Nanoscale*, 2017, **9**(2), 631–636, DOI: 10.1039/c6nr08892a.

105 C. Xu, Z. Liu and E. Lee, High-performance inverted planar perovskite solar cells using a pristine fullerene mixture as an electron-transport layer, *J. Mater. Chem. C*, 2019, **7**(23), 6956–6963, DOI: 10.1039/C9TC01741K.

106 S. Collavini, M. Saliba, W. R. Tress, P. J. Holzhey, S. F. Völker, K. Domanski, S. H. Turren-Cruz, A. Ummadisingu, S. M. Zakeeruddin, A. Hagfeldt, M. Grätzel and J. L. Delgado, Poly(ethylene glycol)-[60] Fullerene-Based Materials for Perovskite Solar Cells with Improved Moisture Resistance and Reduced Hysteresis, *ChemSusChem*, 2018, **11**(6), 1032–1039, DOI: 10.1002/cssc.201702265.

107 J. Pan, S. P. Sarmah, B. Murali, I. Dursun, W. Peng, M. R. Parida, J. Liu, L. Sinatra, N. Alyami, C. Zhao, E. Alarousu, T. K. Ng, B. S. Ooi, O. M. Bakr and O. F. Mohammed, Air-Stable Surface-Passivated Perovskite Quantum Dots for Ultra-Robust, Single- and Two-Photon-Induced Amplified Spontaneous Emission, *J. Phys. Chem. Lett.*, 2015, **6**(24), 5027–5033, DOI: 10.1021/acs.jpclett.5b02460.

108 I. Hwang, I. Jeong, J. Lee, M. J. Ko and K. Yong, Enhancing Stability of Perovskite Solar Cells to Moisture by the Facile Hydrophobic Passivation, *ACS Appl. Mater. Interfaces*, 2015, **7**(31), 17330–17336, DOI: 10.1021/acsami.5b04490.

109 H. Huang, B. Chen, Z. Wang, T. F. Hung, A. S. Susha, H. Zhong and A. L. Rogach, Water resistant CsPbX3 nanocrystals coated with polyhedral oligomeric silsesquioxane and their use as solid state luminophores in all-perovskite white light-emitting devices, *Chem. Sci.*, 2016, **7**(9), 5699–5703, DOI: 10.1039/c6sc01758d.

110 S. Yang, Y. Wang, P. Liu, Y.-B. Cheng, H. J. Zhao and H. G. Yang, Functionalization of perovskite thin films with moisture-tolerant molecules, *Nat. Energy*, 2016, **1**(2), 15016, DOI: 10.1038/nenergy.2015.16.

111 S. N. Raja, Y. Bekenstein, M. A. Koc, S. Fischer, D. Zhang, L. Lin, R. O. Ritchie, P. Yang and A. P. Alivisatos, Encapsulation of Perovskite Nanocrystals into Macroscale Polymer Matrices: Enhanced Stability and Polarization, *ACS Appl. Mater. Interfaces*, 2016, **8**(51), 35523–35533, DOI: 10.1021/acsami.6b09443.

112 M. Meyns, M. Perálvarez, A. H. Jungemann, W. Hertog, M. Ibáñez, R. Nafria, A. Genç, J. Arbiol, M. V. Kovalenko, J. Carreras, A. Cabot and A. G. Kanaras, Polymer-Enhanced Stability of Inorganic Perovskite Nanocrystals and Their Application in Color Conversion LEDs, *ACS Appl. Mater. Interfaces*, 2016, **8**(30), 19579–19586, DOI: 10.1021/acsami.6b02529.

113 Q. Zhou, Z. Bai, W. Lu, Y. Wang, B. Zou and H. Zhong, In Situ Fabrication of Halide Perovskite Nanocrystal-Embedded Polymer Composite Films with Enhanced Photoluminescence for Display Backlights, *Adv. Mater.*, 2016, **28**(41), 9163–9168, DOI: 10.1002/adma.201602651.

114 Z. Chen, Z.-G. Gu, W.-Q. Fu, F. Wang and J. Zhang, A Confined Fabrication of Perovskite Quantum Dots in Oriented MOF Thin Film, *ACS Appl. Mater. Interfaces*, 2016, **8**(42), 28737–28742, DOI: 10.1021/acsami.6b11712.

115 A. Loiudice, S. Saris, E. Oveisi, D. T. L. Alexander and R. Buonsanti, CsPbBr3 QD/AlO x Inorganic Nanocomposites with Exceptional Stability in Water, Light, and Heat, *Angew. Chem., Int. Ed.*, 2017, **56**(36), 10696–10701, DOI: 10.1002/anie.201703703.

116 L. Gomez, C. de Weerd, J. L. Hueso and T. Gregorkiewicz, Color-stable water-dispersed cesium lead halide perovskite nanocrystals, *Nanoscale*, 2017, **9**(2), 631–636, DOI: 10.1039/c6nr08892a.

117 W. Xu, Z. Cai, F. Li, J. Dong, Y. Wang, Y. Jiang and X. Chen, Embedding lead halide perovskite quantum dots in carboxybenzene microcrystals improves stability, *Nano Res.*, 2017, **10**(8), 2692–2698, DOI: 10.1007/s12274-017-1471-0.

118 C. Ma, M.-F. Lo and C.-S. Lee, Stabilization of organometallic halide perovskite nanocrystals in aqueous solutions and their applications in copper ion detection, *Chem. Commun.*, 2018, **54**(45), 5784–5787, DOI: 10.1039/c8cc02221f.

119 D. Zhang, Y. Xu, Q. Liu and Z. Xia, Encapsulation of CH3NH3PbBr3 Perovskite Quantum Dots in MOF-5 Microcrystals as a Stable Platform for Temperature and Aqueous Heavy Metal Ion Detection, *Inorg. Chem.*, 2018, **57**(8), 4613–4619, DOI: 10.1021/acs.inorgchem.8b00355.

120 L.-Q. Lu, M.-Y. Ma, T. Tan, X.-K. Tian, Z.-X. Zhou, C. Yang and Y. Li, Novel dual ligands capped perovskite quantum dots for fluoride detection, *Sens. Actuators, B*, 2018, **270**, 291–297, DOI: 10.1016/j.snb.2018.05.038.

121 T. Kokulnathan and T.-J. Wang, Synthesis and characterization of 3D flower-like nickel oxide entrapped on boron doped carbon nitride nanocomposite: An efficient catalyst for the electrochemical detection of nitrofurantoin, *Composites, Part B*, 2019, 106914, DOI: 10.1016/j.compositesb.2019.106914.

122 T. Kokulnathan, V. Suvina, T. Wang and R. G. Balakrishna, Synergistic design of a tin phosphate-entrapped graphene flake nanocomposite as an efficient catalyst for electrochemical determination of the antituberculosis drug isoniazid in biological samples, *Inorg. Chem. Front.*, 2019, **6**(7), 1831–1841, DOI: 10.1039/C9QI00254E.

123 V. Suvina, S. Murali Krishna, D. H. Nagaraju, J. S. Melo and R. Geetha Balakrishna, Polypyrrole-reduced graphene oxide nanocomposite hydrogels: A promising electrode material for the simultaneous detection of multiple heavy metal ions, *Mater. Lett.*, 2018, **232**, 209–212, DOI: 10.1016/j.matlet.2018.08.096.

124 V. Suvina, T. Kokulnathan, T.-J. Wang and R. G. Balakrishna, Unraveling the electrochemical properties of lanthanum cobaltite decorated halloysite nanotube nanocomposite: An advanced electrocatalyst for

determination of flutamide in environmental samples, *Ecotoxicol. Environ. Saf.*, 2020, **190**, 110098, DOI: 10.1016/j.ecoenv.2019.110098.

125 D. Guziejewski, Square-wave amplitude effect in cathodic and anodic stripping square-wave voltammetry, *Electroanalysis*, 2019, **31**(2), 231–238, DOI: 10.1002/elan.201800425.

126 Y. Shimizu, S. Yamamoto and S. Takase, A thick-film impedancemetric carbon monoxide sensor using layered perovskite-type cuprate, *Sens. Actuators, B*, 2017, **249**, 667–672, DOI: 10.1016/j.snb.2017.04.059.

127 N. F. Atta, E. H. El-Ads, A. Galal and A. E. Galal, Electrochemical sensing platform based on nano-perovskite/glycine/carbon composite for amlodipine and ascorbic acid drugs, *Electroanalysis*, 2019, **31**(3), 448–460, DOI: 10.1002/elan.201800577.

128 Z. Anajafi, M. Naseri, S. Marini, C. Espro, D. Iannazzo, S. G. Leonardi and G. Neri, $NdFeO_3$ as a new electrocatalytic material for the electrochemical monitoring of dopamine, *Anal. Bioanal. Chem.*, 2019, **411**, 7681–7688, DOI: 10.1007/s00216-019-01975-z.

129 J. He, J. Sunarso, J. Miao, H. Sun, J. Dai, C. Zhang, W. Zhou and Z. Shao, A highly sensitive perovskite oxide sensor for detection of p-phenylenediamine in hair dyes, *J. Hazard. Mater.*, 2019, **369**, 699–706, DOI: 10.1016/j.jhazmat.2019.02.070.

130 P. Sundaresan, R. Karthik, S. M. Chen, J. Vinoth Kumar, V. Muthuraj and E. R. Nagarajan, Ultrasonication-assisted synthesis of sphere-like strontium cerate nanoparticles (SrCeO3 NPs) for the selective electrochemical detection of calcium channel antagonists nifedipine, *Ultrason. Sonochem.*, 2019, **53**, 44–54, DOI: 10.1016/j.ultsonch.2018.12.013.

131 B. Muthukutty, R. Karthik, S. Chen and M. Abinaya, Designing novel perovskite-type strontium stannate ($SrSnO_3$) and its potential as an electrode material for the enhanced sensing of anti-inflammatory drug mesalamine in biological samples, *New J. Chem.*, 2019, **43**, 12264–12274, DOI: 10.1039/C9NJ02197C.

132 A. Muthumariyappan, U. Rajaji, S. M. Chen, N. Baskaran, T. W. Chen and R. Jothi Ramalingam, Sonochemical synthesis of perovskite-type barium titanate nanoparticles decorated on reduced graphene oxide nanosheets as an effective electrode material for the rapid determination of ractopamine in meat samples, *Ultrason. Sonochem.*, 2019, **56**, 318–326, DOI: 10.1016/j.ultsonch.2019.04.005.

133 S. M. Ali and H. A. Al lehaibi, Smart Perovskite Sensors: The Electrocatalytic Activity of SrPdO3for Hydrazine Oxidation, *J. Electrochem. Soc.*, 2018, **165**(9), B345–B350, DOI: 10.1149/2.0221809jes.

134 R. Ramachandran, T. Chen, S. Chen, T. Baskar, R. Kannan, P. Elumalai, P. Raja, T. Jeyapragasam, K. Dinakaran and G. P. Gnana kumar, A review of the advanced developments of electrochemical sensors for the detection of toxic and bioactive molecules, *Inorg. Chem. Front.*, 2019, **6**(12), 3418–3439, DOI: 10.1039/C9QI00602H.

135 T. Vijayaraghavan, R. Sivasubramanian, S. Hussain and A. Ashok, A Facile Synthesis of LaFeO3 -Based Perovskites and Their Application towards Sensing of Neurotransmitters, *ChemistrySelect*, 2017, **2**(20), 5570–5577, DOI: 10.1002/slct.201700723.

136 S. Akbari, M. M. Foroughi, H. H. Nadiki and S. Jahani, Synthesis and characterization of LaMnO3 nanocrystals and graphene oxide: fabrication of graphene oxide–LaMnO3 sensor for simultaneous electrochemical determination of hydroquinone and catechol, *J. Electrochem. Sci. Eng.*, 2019, **9**, 255–267, DOI: 10.5599/jese.634.

137 F. Cao, Q. Dong, C. Li, J. Chen, X. Ma, Y. Huang, D. Song, C. Ji and Y. Lei, Electrochemical sensor for detecting pain reliever/fever reducer drug acetaminophen based on electrospun CeBiO x nanofibers modified screen-printed electrode, *Sens. Actuators, B*, 2018, **256**, 143–150, DOI: 10.1016/j.snb.2017.09.204.

138 K. Ahmad, P. Kumar and S. M. Mobin, A highly sensitive and selective hydroquinone sensor based on a newly designed N-rGO/SrZrO3 composite, *Nanoscale Adv.*, 2020, **2**(1), 502–511, DOI: 10.1039/C9NA00573K.

139 M.-A. Stoeckel, M. Gobbi, S. Bonacchi, F. Liscio, L. Ferlauto, E. Orgiu and P. Samorì, Reversible, Fast, and Wide-Range Oxygen Sensor Based on Nanostructured Organometal Halide Perovskite, *Adv. Mater.*, 2017, **29**(38), 1702469, DOI: 10.1002/adma.201702469.

140 G. Kakavelakis, E. Gagaoudakis, K. Petridis, V. Petromichelaki, V. Binas, G. Kiriakidis and E. Kymakis, Solution Processed CH3NH3PbI3−xClx Perovskite Based Self-Powered Ozone Sensing Element Operated at Room Temperature, *ACS Sens.*, 2017, **3**(1), 135–142, DOI: 10.1021/acssensors.7b00761..

141 A. Natkaeo, D. Phokharatkul, J. H. Hodak, A. Wisitsoraat and S. K. Hodak, Highly selective sub–10 ppm H 2 S gas sensors based on Ag-doped CaCu 3 Ti 4 O 12 films, *Sens. Actuators, B*, 2018, **260**, 571–580, DOI: 10.1016/j.snb.2017.12.134.

142 H. Zhang, J. Yi and X. Jiang, Fast Response, Highly Sensitive and Selective Mixed-Potential H2 Sensor Based on (La, Sr)(Cr, Fe)O3-δ Perovskite Sensing Electrode, *ACS Appl. Mater. Interfaces*, 2017, **9**(20), 17218–17225.

143 Y. Shimizu, S. Yamamoto and S. Takase, A thick-film impedancemetric carbon monoxide sensor using layered perovskite-type cuprate, *Sens. Actuators, B*, 2017, **249**, 667–672, DOI: 10.1016/j.snb.2017.04.059.

144 L. Dou, Y. Yang, J. You, Z. Hong, W. H. Chang, G. Li, and Y. Yang, Solution-processed hybrid perovskite photodetectors with high detectivity, *Nat. Commun.*, 2014, **5**, 5404, DOI: 10.1038/ncomms6404.

145 V. W. T. Liu and P. L. Huang, Cardiovascular roles of nitric oxide: a review of insights from nitric oxide synthase gene disrupted mice, *Cardiovasc. Res.*, 2008, **77**(1), 19–29, DOI: 10.1016/j.cardiores.2007.06.024.

146 D. A. Wink, H. B. Hines, R. Y. S. Cheng, C. H. Switzer, W. F. Santana, M. P. Vitek, L. A. Ridnour and C. A. Colton, Nitric oxide and redox mechanisms in the immune

response, *J. Leukocyte Biol.*, 2011, **89**(6), 873–891, DOI: 10.1189/jlb.1010550.

147 V. L. Dawson and T. M. Dawson, Nitric oxide in neurodegeneration, in *Progress in Brain Research*, ed. R. R. Mize, T. M. Dawson, V. L. Dawson and M. J. Friedlander, Elsevier, 1998, ch. 15, vol. 118, pp. 215–229. DOI: 10.1016/S0079-6123(08)63210-0.

148 R. Zhu, Y. Zhang, H. Zhong, X. Wang, H. Xiao, Y. Chen and X. Li, High-performance room-temperature NO_2 sensors based on $CH_3NH_3PbBr_3$ semiconducting films: Effect of surface capping by alkyl chain on sensor performance, *J. Phys. Chem. Solids*, 2019, **129**, 270–276, DOI: 10.1016/j.jpcs.2019.01.020.

149 J. Wang, C. Wang, A. Liu, R. You, F. Liu, S. Li, L. Zhao, R. Jin, J. He, Z. Yang, P. Sun, X. Yan and G. Lu, High-response mixed-potential type planar YSZ-based NO_2 sensor coupled with $CoTiO_3$ sensing electrode, *Sens. Actuators, B*, 2019, **287**, 185–190, DOI: 10.1016/j.snb.2019.02.005.

150 X. D. Zhang, W. L. Zhang, Z. X. Cai, Y. K. Li, Y. Yamauchi and X. Guo, $LaFeO_3$ porous hollow micro-spindles for NO_2 sensing, *Ceram. Int.*, 2019, **45**(5), 5240–5248, DOI: 10.1016/j.ceramint.2018.11.221.

151 X. Li, L. Dai, Z. He, W. Meng, Y. Li and L. Wang, In situ exsolution of PdO nanoparticles from non-stoichiometric LaFePd0.05O3+ δ electrode for impedancemetric NO2 sensor, *Sens. Actuators, B*, 2019, **298**, 126827, DOI: 10.1016/j.snb.2019.126827.

152 G. Cai, J. Cong, C. Zhang, Y. Zheng, F. Zhong, Y. Xiao and L. Jiang, Cu incorporated perovskite Na0.5Bi0.5TiO3 oxygen-defect conductor as NO2 sensor using CuO sensitive electrode, *Ceram. Int.*, 2019, **45**, 8494–8503, DOI: 10.1016/j.ceramint.2019.01.161.

153 Y. Zhuang, W. Yuan, L. Qian, S. Chen and G. Shi, High-performance gas sensors based on a thiocyanate ion-doped organometal halide perovskite, *Phys. Chem. Chem. Phys.*, 2017, **19**(20), 12876–12881, DOI: 10.1039/c7cp01646h.

154 G. Lu, Q. Diao, C. Yin, S. Yang, Y. Guan, X. Cheng and X. Liang, High performance mixed-potential type NOx sensor based on stabilized zirconia and oxide electrode, *Sens. Actuators, B*, 2014, **262**, 292–297, DOI: 10.1016/j.ssi.2014.01.037.

155 N. Sharma, H. S. Kushwaha, S. K. Sharma and K. Sachdev, Fabrication of $LaFeO_3$ and rGO-$LaFeO_3$ microspheres based gas sensors for detection of NO_2 and CO, *RSC Adv.*, 2020, **10**(3), 1297–1308, DOI: 10.1039/C9RA09460A.

156 S. Chakraborty and M. Pal, Highly efficient novel carbon monoxide gas sensor based on bismuth ferrite nanoparticles for environmental monitoring, *New J. Chem.*, 2018, **42**(9), 7188–7196, DOI: 10.1039/c8nj01237g.

157 K. C. Hsu, T. H. Fang, Y. J. Hsiao and P. C. Wu, Response and characteristics of TiO_2/perovskite heterojunctions for CO gas sensors, *J. Alloys Compd.*, 2019, **794**, 576–584, DOI: 10.1016/j.jallcom.2019.04.238.

158 H. Zhang, J. Yi and X. Jiang, Fast Response, Highly Sensitive and Selective Mixed-Potential H2 Sensor Based on (La, Sr)(Cr, Fe)O3-δ Perovskite Sensing Electrode, *ACS Appl. Mater. Interfaces*, 2017, **9**(20), 17218–17225, DOI: 10.1021/acsami.7b01901.